Text and references accompanying Nevada Bureau of Mines and Geology Map 189

Geologic Map of the Secret Valley Quadrangle, Elko County, Nevada

by

Arthur W. Snoke[1], Keith A. Howard[2], and Seth Dee[3]

[1]University of Wyoming, Laramie, WY
[2]U.S. Geological Survey, Mountain View, CA
[3]Nevada Bureau of Mines and Geology, University of Nevada, Reno

2021

Disclaimer: This geologic map was funded in part by the USGS National Cooperative Geologic Mapping Program under STATEMAP award number G19AC00383, 2020.

ABSTRACT

The map units in the Secret Valley quadrangle range from Holocene to Neoproterozoic in age. The map area provides exceptional exposures of a west-rooted, (i.e., originally west-dipping), normal-sense late Oligocene mylonitic shear zone (~1+ km thick) and an associated middle Miocene (17–15 Ma) detachment-fault system. These characteristic structural features are important components of the Ruby Mountains–East Humboldt Range (RM-EHR) core complex. The detachment-fault system, including fault-bounded slices of distinctive Devonian to Ordovician units (Dg, DOd, Oe, and Olm), separates a hanging wall of chiefly unmetamorphosed Lower Triassic and upper Paleozoic sedimentary rocks and middle Eocene volcanic and volcaniclastic rocks from a footwall of metamorphosed middle Paleozoic to Neoproterozoic metasedimentary rocks. This footwall contains a unit of Cambrian–Neoproterozoic Prospect Mountain Quartzite and the Neoproterozoic McCoy Creek Group (Ꞓ€Zpmi), and a unit consisting chiefly of Ordovician–Cambrian calcite marble and calc-silicate rocks (O€mi). The footwall rocks are commonly mylonitic.

Deformed intrusive rocks are common throughout the footwall map units. These intrusive rocks occur as thin (<1–3 m), sheet-like to irregular bodies that have sharp contacts with their host metamorphic rocks. An extended range in composition from mafic to felsic characterizes these igneous rocks. Typical examples are gabbro–quartz diorite, biotite granodiorite–monzogranite orthogneiss, and muscovite leucogranite orthogneiss. Similar intrusive rocks occur in the adjacent Gordon Creek quadrangle and have been dated as middle Eocene. Pegmatitic leucogranite is also widespread in the footwall units and is correlated with early Oligocene–Late Cretaceous leucogranite common throughout the RM-EHR core complex. Small areas of granitic orthogneiss of Secret Peak, biotite-muscovite monzogranitic orthogneiss, and quartz diorite of Rattlesnake Canyon are locally mapped separately.

The unmetamorphosed strata of the hanging wall include rocks ranging from the Pennsylvanian–Mississippian Diamond Peak Formation to the Early Triassic Thaynes Formation. One small exposure of middle Eocene volcanic and volcaniclastic rocks is also part of the hanging-wall sequence. Various paleontological age data have been determined from the unmetamorphosed sedimentary sequence, including from megafossils, fusulinids, and conodonts. The conodonts provide age determinations and thermal histories through conodont alteration indices (CAIs). High CAIs (5–6) from the Pennsylvanian Ely Limestone (IPe) indicate that the host rock reached 400–500 ºC. These temperature determinations are interpreted to be related to hot fluids generated from the metamorphic and igneous footwall of the detachment-fault system.

The metamorphic and igneous complex forming the footwall records a complex history of penetrative deformation, polyphase folding, and crystal-plastic deformation in the mylonitic shear zone. Pre-mylonitic folds are well-developed in the southwestern corner of the quadrangle. These folds typically fold an earlier foliation with hinge lines trending to the northwest–southeast and are locally overprinted by the mylonitic shear zone. The formation age of the pre-mylonitic foliation and folds is uncertain, but it may be Late Cretaceous synchronous with upper-amphibolite facies metamorphism dated by U-Pb on monazite. Upper-amphibolite facies conditions for the metamorphic rocks of the footwall are based on the presence of the metapelitic assemblage: quartz + biotite + sillimanite + plagioclase + muscovite + garnet + zircon. Two metapelite

samples from the southwestern corner of the Secret Valley quadrangle in the ЄZpmi unit yielded ~4 kb and ~600 ºC for the P–T (pressure and temperature) conditions based on thermobarometric data during regional metamorphism. Calc-silicate rocks having hornblende + diopside + garnet assemblages also support upper-amphibolite facies conditions for the metamorphism of the metasedimentary rocks. U-Pb monazite ages from the ЄZpmi unit suggest a Late Cretaceous age for the upper-amphibolite facies metamorphism.

The younger mylonitic shear zone is characterized by a penetrative foliation and elongation lineation (stretching lineation) that typically trends west-northwest–east-southeast. Locally, this lineation is folded by post-mylonitic folds that typically show vergence to the west. These folds are interpreted as Oligocene and related to the shear deformation characteristic of the mylonitic shear zone. Microstructures in the mylonitic rocks such as grain-boundary migration, subgrain rotation, recrystallization of quartz, and asymmetric porphyroclasts indicate crystal-plastic deformation. Thermobarometric data from mylonitic rocks in the adjacent Tent Mountain quadrangle indicate P–T conditions of 3.1–3.7 kb and 580–620 ºC. Mylonitization ended by ~29–23 Ma based on published geochronologic and thermochronologic data. Thus, age and P–T estimates suggest that the metamorphic rocks in the Secret Valley quadrangle reflect upper-amphibolite facies metamorphism in the Late Cretaceous followed by early Oligocene mylonitization. The mylonitic shear zone was interpreted to reflect an early part of exhumation of the footwall of the detachment-fault zone.

Scarce outcrops of the middle Miocene Humboldt Formation are mapped in the northwestern corner of the quadrangle. Associated with the Humboldt Formation are rhyolite exposures, including a vitrophyre that yielded a date of 15 ± 1.5 Ma by the K-Ar technique on sanidine and a rhyolite flow that yielded an $^{40}Ar/^{39}Ar$ age of 15.37 Ma on anorthoclase (see table 1).

Small exposures of Humboldt Formation are poorly exposed along the southwest margin of Secret Valley and in north Ruby Valley suggesting that the Humboldt Formation underlies these topographic features. Exposures of the Humboldt Formation, more extensively exposed in the adjacent Heelfly Creek quadrangle, have been mapped as unconformably deposited on Paleozoic sedimentary rocks as well as units in the metamorphic and igneous complex. The basal contact of the Humboldt Formation in the Secret Valley quadrangle is poorly exposed. However, based on the geologic mapping in the Heelfly Creek quadrangle, it is also mapped here as an unconformity. If this is the correct interpretation, the RM-EHR detachment fault and mylonitic shear zone were denuded prior to the middle Miocene. Cobbles of metasedimentary and deformed metaigneous rocks in the Humboldt Formation support this interpretation.

Normal faults accommodate offset of the mylonitic shear zone as well as the RM-EHR detachment-fault zone. A normal fault is exposed east of Secret Pass in the 'Secret Hills'. This unnamed fault accommodated downdrop of the undivided Lower Permian sedimentary rocks in the hanging wall of the RM-EHR detachment fault. This fault loses displacement farther north in Secret Valley. The Poison Canyon fault is an en echelon normal fault that is the important range-front normal fault in the Secret Valley quadrangle. It is estimated that the Poison Canyon fault has about one km of displacement along it. It can be traced north into the Tent Mountain quadrangle, where it loses displacement. These normal faults are interpreted to be post-Humboldt Formation (middle Miocene).

The youngest map units in the Secret Valley quadrangle include a variety of Quaternary deposits: alluvial-fan and stream deposits (Qfy, Qfi, Qfo, and QToa), glacial deposits (Qgm and Qgo), colluvium (Qc), and landslide deposits (Qls).

INTRODUCTION

The Secret Valley quadrangle is situated between the southwestern flank of the East Humboldt Range, the northeastern flank of the Ruby Mountains, and intervening valleys (fig. 1). Secret Valley, a small intermontane valley occupying the center of the quadrangle, is located about 36 km (~22.5 mi) south-southwest of Wells, Nevada. Secret Pass in the central part of the quadrangle marks a low drainage divide separating internally drained Ruby Valley to the south from Secret Valley, which drains northwestward toward the Humboldt River. Surficial deposits in the Secret Creek gorge area suggest that the Secret Valley catchment was integrated into the Humboldt River basin in the middle to late Pleistocene. Qfo fan deposits, of probable middle Pleistocene age, perched just south of the gorge include subrounded to subangular clasts of fanglomorate material sourced from the proximal highlands. A small percentage of these clasts are rhyolite (Tr) sourced from outcrops only present on the northern side of Secret Creek, which requires incision of the gorge to post-date deposition of the Qfo fans. The relatively recent integration of Secret Valley is further supported by pervasive landslides in the Secret Valley drainage catchment, which likely resulted from rapid post-integration incision and slope destabilization. Secret Valley and northern Ruby Valley are underlain by Quaternary deposits.

Scattered exposures of middle Miocene Humboldt Formation adjacent to Secret Valley and northern Ruby Valley suggest that this formation is widely present under both of these topographic features. A small area of Humboldt Formation is exposed at the northwesternmost corner of the quadrangle. The same Miocene rocks are more extensively exposed in the adjacent Heelfly Creek quadrangle area, where Dee et al. (2015) mapped them as unconformable on subjacent unmetamorphosed and metamorphosed Paleozoic rocks.

A system of N–S-striking range-front faults bounds the east flank of the northern Ruby Mountains and is manifested by the Poison Canyon fault, which continues north into the Tent Mountain quadrangle where it gradually loses displacement. A geologic highlight of this quadrangle is the

Ruby Mountains–East Humboldt Range (RM-EHR) detachment-fault system (Snoke, 1980) and an associated 1+-km-thick mylonitic shear zone (Oligocene, Wright and Snoke, 1993). The age of the detachment-fault system post-dates the early Oligocene but pre-dates the middle Miocene (age of the Humboldt Formation). The extensional, normal-sense detachment fault zone and mylonitic shear zone formed as major elements in the evolution of the RM-EHR core complex (Howard, 1980, Snoke, 1980, Snoke et al., 1990; Snoke et al., 1997; Sullivan and Snoke, 2007).

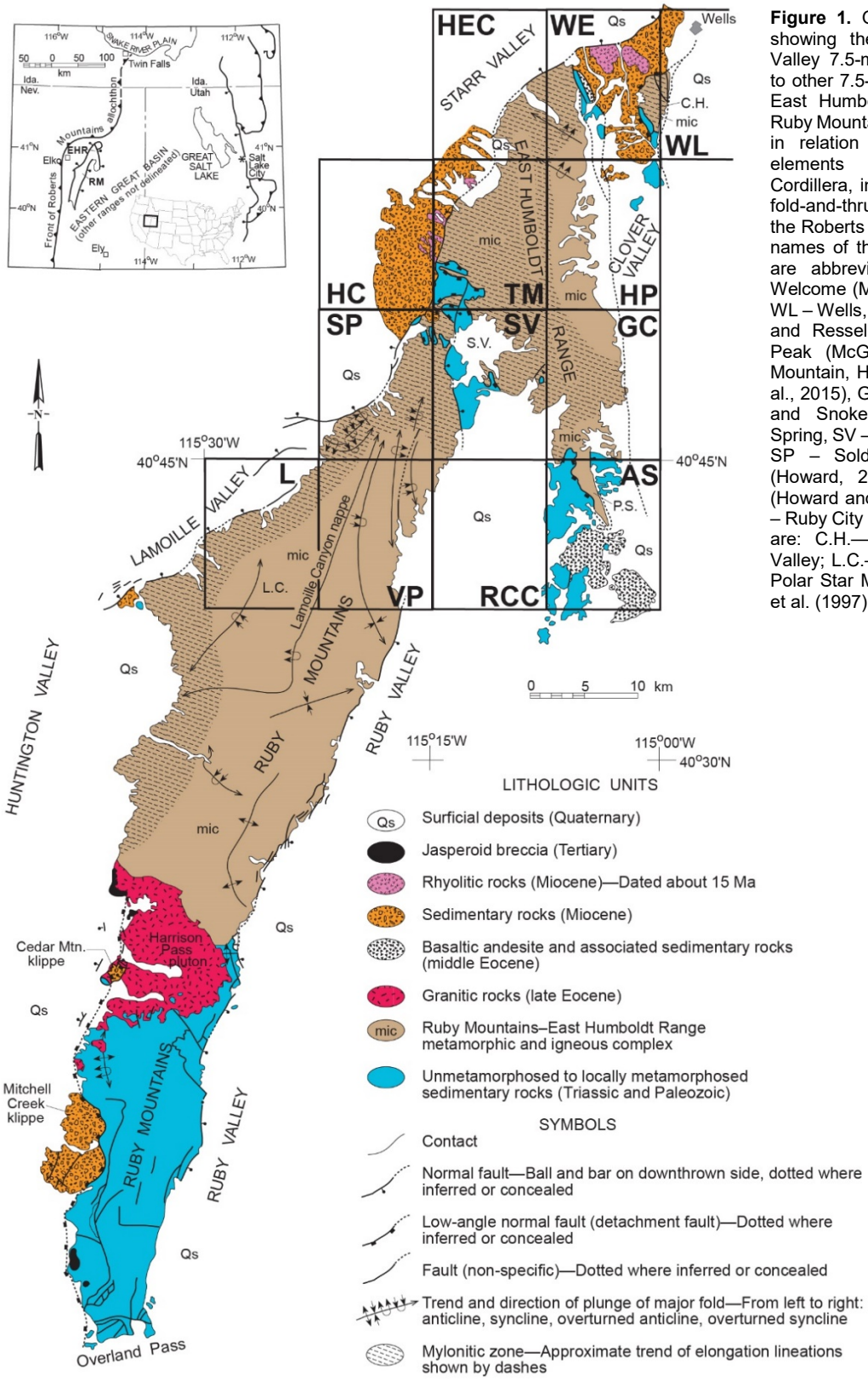

Figure 1. Generalized geologic map showing the location of the Secret Valley 7.5-minute quadrangle relative to other 7.5-minute quadrangles in the East Humboldt Range and northern Ruby Mountains. Inset shows map area in relation to other major tectonic elements of the western U.S. Cordillera, including part of the Sevier fold-and-thrust belt and leading edge of the Roberts Mountains allochthon. The names of the 7.5-minute quadrangles are abbreviated as follows: WE – Welcome (McGrew and Snoke, 2015), WL – Wells, HEC – Herder Creek (Dee and Ressel, 2016), HP – Humboldt Peak (McGrew, 2018), TM – Tent Mountain, HC – Heelfly Creek (Dee et al., 2015), GC – Gordon Creek (Sicard and Snoke, 2020), AS – Arizona Spring, SV – Secret Valley (this report), SP – Soldier Peak, L – Lamoille (Howard, 2000), VP – Verdi Peak (Howard and MacCready, 2004), RCC – Ruby City Creek. Other abbreviations are: C.H.—Clover Hill; S.V.—Secret Valley; L.C.—Lamoille Canyon; P.S.—Polar Star Mine. Modified from Snoke et al. (1997) and Colgan et al. (2010).

The rock units in the Secret Valley quadrangle can broadly be divided into four distinct groups: (1) surficial deposits, including alluvial deposits (Qfy, Qfi, Qfo, and QToa), glacial deposits (Qgo and Qgm), and other surficial deposits (Qc and Qls); (2) unmetamorphosed Tertiary and Mississippian to Lower Triassic stratigraphic units; (3) metamorphosed sedimentary rocks (Neoproterozoic to Upper Devonian); and (4) numerous intrusive igneous rocks that range in age from middle Eocene or early Oligocene to Late Jurassic.

The metamorphosed rocks range in grade from lower greenschist facies (e.g., Olm) to upper-amphibolite facies (sillimanite-muscovite zone, ЄZpmi). The Pennsylvanian Ely Limestone (ℙe) locally occurs as a very low-grade calcite marble with lenticular metachert. Conodont elements from meta-limestone from this unit yield conodont-alteration indices (CAIs) of 5 to 6, indicating that the host rock reached 300 to 400 ºC. These elevated CAIs are interpreted here to be related to hot fluids generated from the metamorphic and igneous footwall of the detachment-fault system.

PREVIOUS WORK

The earliest systematic reports of the geology of the Ruby Mountains and East Humboldt Range date from the 40th Parallel Survey led by Clarence King (1878). It was also the focus of early studies on Basin-and-Range structure and geomorphology (Sharp, 1939, 1940). Prior to our study, the general geology of the northern Ruby Mountains and East Humboldt Range was mapped by Snelson (1957), who recognized unmetamorphosed upper Paleozoic formations in the southwest part of the quadrangle and mapped a low-angle fault in the Secret Pass area. Snelson (1957) interpreted this fault as an east-directed thrust fault (i.e., his Secret Creek thrust), which separated unmetamorphosed middle to upper Paleozoic rocks from a subjacent metamorphosed footwall. He also interpreted east-dipping faults along the eastern flank of the northern Ruby Mountains as part of his Secret Pass thrust fault. Snelson (1957) subdivided the metamorphic rocks into the Angel Lake and Snow Water units, based on differences in rock types, metamorphism, mylonization, and migmatization. In the Secret Valley quadrangle, he also interpreted the contact between the overlying Snow Water unit and subjacent Angel Lake unit as a thrust fault. Snelson (1957) interpreted the Secret Creek thrust to be Mesozoic in age that emplaced younger rocks on older rocks. Howard (1966, 1971, 1980) and Howard et al. (1979) correlated metamorphosed strata in the northern Ruby Mountains to Paleozoic and Neoproterozoic units and reconnoitered parts of the quadrangle. Snoke (1980 and later publications) established that Snelson's Secret Creek thrust is instead a low-angle normal fault, part of the RM-EHR detachment-fault system (see also McGrew and Snoke, 2015; McGrew, 2018, and Sicard and Snoke, 2020).

STRUCTURAL GEOLOGY

The Secret Valley quadrangle exposes a detailed cross section through the RM-EHR normal-sense detachment-fault system (see cross section A–A'). The fault zone is characterized by fault-bounded slices of the miogeoclinal strata of the eastern Great Basin. Some slices are metamorphosed whereas others are not. The unmetamorphosed sedimentary rocks are cut by normal faults that are supposed on a brittle, low-angle detachment-fault zone over the metamorphic and igneous footwall. Plastic-to-brittle low-angle faults (change from crystal-plastic deformation to brittle fracture during exhumation) commonly bound the base of slices of metamorphosed strata including Olm, Oe, DOd, and Dg units. The fault slice of metamorphosed Lehman Formation (Olm) occurs below a slice of the dolomitic marble (DOd), in a younger-on-older relationship. In the Secret Creek gorge area in the northwest part of the quadrangle, a plastic-to-brittle low-angle fault, which varies from concordant to discordant with respect to the underlying ЄZpmi unit, superposes the OЄmi unit against the ЄZpmi unit.

An unusual older-on-younger relationship occurs in part of the RM-EHR detachment-fault zone at T. 34 N, R. 60 E, NE quarter of section 13. There, several small outcrops of mylonitic metaconglomerate of the Pennsylvanian–Mississippian Diamond Peak Formation (Mdp, only one outcrop is mapped) are structurally above strongly mylonitic orthogneisses of the OЄmi unit and structurally below needby klippen of Oe. The occurrences of older rocks above younger rocks are rare in the detachment-fault zone. Snoke (1980, his fig. 5) documented older-on-younger fault relationships in the Tent Mountain quadrangle, immediately north of the Secret Valley quadrangle, where Diamond Peak Formation and Ely Limestone are structurally above a window of Lower Permian rocks. The more common structural sequence is younger rocks emplaced on older rocks, such that the whole Paleozoic stratigraphic section is dramatically thinned by plastic-to-brittle deformation. The rarer older-on-younger relationship suggests that the original structural stack may have included older-on-younger thrust plates that were subsequently dismembered by extensional faulting along the Tertiary RM-EHR detachment-fault zone. The footwall to these fault-bounded slices are the OЄmi and ЄZpmi units.

The RM-EHR detachment-fault zone overprints a related mid-Tertiary extensional mylonitic shear zone based on structural relationships and U-Pb geochronology. The age of the mylonitic shear zone is roughly bracketed to have ended between 29 and 23 Ma (late Oligocene; Dokka et al., 1986 [fission-track, apatite, zircon, and titanite]; Dallmeyer et al., 1986 [$^{40}Ar/^{39}Ar$ dating, hornblende and biotite]; Wright and Snoke, 1993 [U-Pb igneous ages, zircon]). Hurlow et al. (1991) estimated pressure and temperature conditions of the mylonitization in the adjacent Tent Mountain quadrangle as 3.1–3.7 kb and 580–620 ºC, based on geothermobarometry of a pelitic schist from the mylonitic shear zone. These authors concluded that the shear zone–

Figure 2. Mylonitic migmatitic impure metaquartzite, orthogneiss (massive layer in the center of photograph with leucosome layer), and schist of the €Zpmi unit. Note the small-scale interlayering of orthogneiss and biotite feldspathic metaquartzite in the lower left corner of the photograph. The complete transposition of all compositional layering is characteristic of rocks in the mylonitic shear zone.

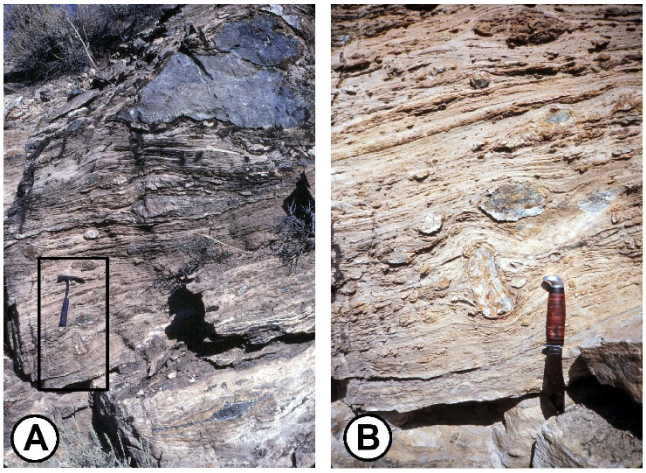

Figure 3. Mylonitic marbles in the O€mi unit. A. Mylonitic calcite marble containing various competent clasts. The large massive clast in the upper part of the photograph is hornblende gabbro of probable middle Eocene age. Similar gabbroic rocks have been dated in the East Humboldt Range as middle Eocene (~38–40 Ma) (Wright and Snoke, 1993). The rectangle box outlines the area of photograph B. B. Close-up of part of the outcrop in A (lower left below hammer handle). Rotated clast of competent paragneiss (left of knife handle) in mylonitic calcite marble. Note that a mylonitic fluxion structure is deflected around the clast, which itself contains a mylonitic foliation. Both foliations developed during a continuous noncoaxial deformation.

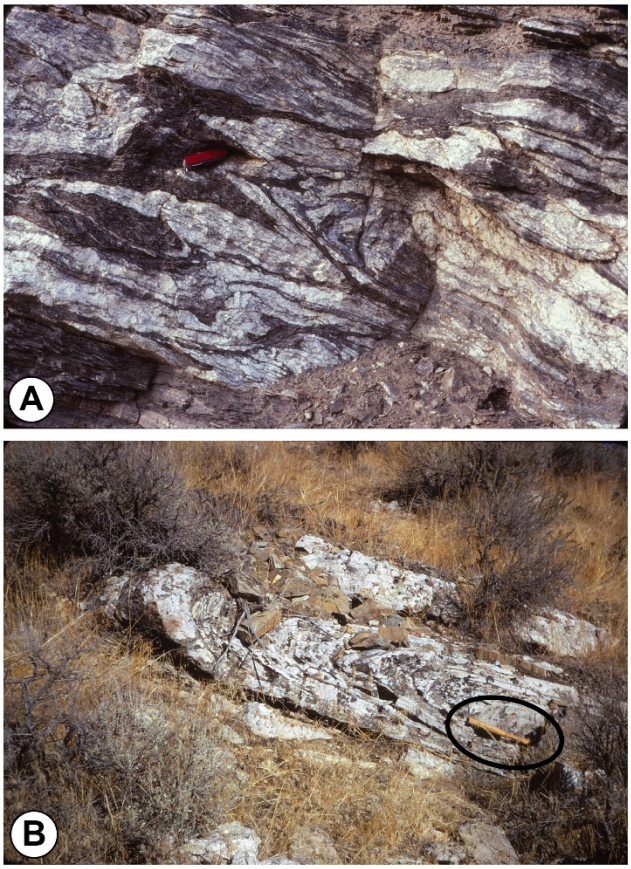

Figure 4. Westward vergent post-mylonitic (Tertiary) folds. A. Tightly folded interlayered pelitic schist and mylonitic leucogranite. Note that the mylonitic foliation in the leucogranite is folded. Foliation in the pelitic schist in the hinge zone of the folds has been rotated subparallel to the axial surfaces of the folded leucogranite layers. Note pen knife for scale. B. An overturned isoclinal fold in mylonitic white metaquartzite of the O€mi unit. This northwest-vergent fold displays rotation of an earlier pervasive mylonitic elongation lineation during late folding in the mylonitic shear zone. Note inclined hammer (within oval) in lower left corner of the photograph for scale.

detachment-fault system excised 11–12 km of crustal section and accommodated at least 15–17 km of normal-sense dip slip, top to the west. Middle Miocene Humboldt Formation and an associated ~15-Ma rhyolite flow (see table 1 for details about the age of this unit) occur as an unconformable stratigraphic sequence deposited on Paleozoic unmetamorphosed and metamorphosed rocks of the RM-EHR detachment-fault system (Dee et al., 2015; this report). This stratigraphic relationship conclusively indicates that detachment-fault system developed prior to 15 Ma. However, in the Tent Mountain quadrangle, a ~17-Ma basalt dike is truncated by a low-angle fault, with unmetamorphosed Lower Permian rocks in the hanging wall, considered to be part of the RM-EHR detachment-fault system (Snoke, 1980, his figure 5). Clasts of metamorphosed Eureka Quartzite, calcite marble, and mylonitic leucogranitic orthogneiss in the Humboldt Formation indicate that the metamorphic and igneous substratum was exposed by middle Miocene time (Snoke, 1980; Snoke, unpublished data from the Soldier Peak quadrangle; Dee et al., 2015). Retrogressive mineral assemblages in mylonitic orthogneisses, below the brittle detachment fault, indicate that displacement along this low-angle fault occurred after the development of the mylonitic shear zone, which is documented as late Oligocene by Wright and Snoke (1993). These data suggest that the age of the RM-EHR detachment-fault zone in the Secret Creek gorge area is tightly bracketed between ~17–15 Ma (middle Miocene). This relationship is older than younger low-angle detachment faulting in the Welcome quadrangle in the northern East Humboldt Range (McGrew and Snoke, 2015). In that area, middle Miocene

Humboldt Formation occurs in the hanging wall of the brittle detachment fault and tilted rocks as young as ~8–10 Ma are part of the extensional allochthon (Mueller, 1992).

Mylonitic rocks are spectacularly exposed in the O€mi and €Zpmi units (figs. 2, 3, and 4) and are especially well-exposed in the Secret Creek gorge area in the northwest corner of the quadrangle (Snoke and Howard, 1984; Snoke et al., 1997; Snoke, 1998). The mylonitic rocks, especially the granitic rocks and metaquartzites, are characterized by a pervasive elongation (stretching) lineation that trends from west-northwest to northwest and east-southeast to southeast. These mylonitic rocks exhibit various sense-of-shear features such as S-C fabric in granitic rocks and oblique foliations in metaquartzites (both types 1 and 2, respectively, of Lister and Snoke, 1984). Other sense-of-shear features include asymmetric mantled porphyroclasts, mica fish, and the vergence of post-mylonitic folds (figs. 4A, B). The predominant sense-of-shear is to top to the west-northwest to northwest indicating a west-rooted mylonitic shear zone. This includes many eastward-dipping exposures of the mylonitic rocks where the sense-of-shear is up the trend and plunge of the mylonitic elongation lineation, indicating the west-rooted mylonitic shear zone has been warped or tilted during its development (Spencer, 1984). The mylonitic shear zone has a thickness of ~1 km. Mylonitic fabrics exposed in upper-amphibolite facies metamorphic rocks in the southwest part of the quadrangle decrease in intensity structurally downward toward lower elevations.

Structural attitudes collected during the geologic mapping of the Secret Valley quadrangle are summarized in figure 5. Figure 5A shows the distribution of bedding attitudes from unmetamorphosed sedimentary rocks (Ŧt–ℙMdp) exposed in the northeastern Ruby Mountains above the RM-EHR detachment fault (see cross section A–A'). The poles to bedding are scattered in the NW–N part of the equal-area, stereographic net, but a best-fit great circle with an average fold axis of 41º/135º (p/t) can be inferred from the data. The distribution of the bedding readings indicates

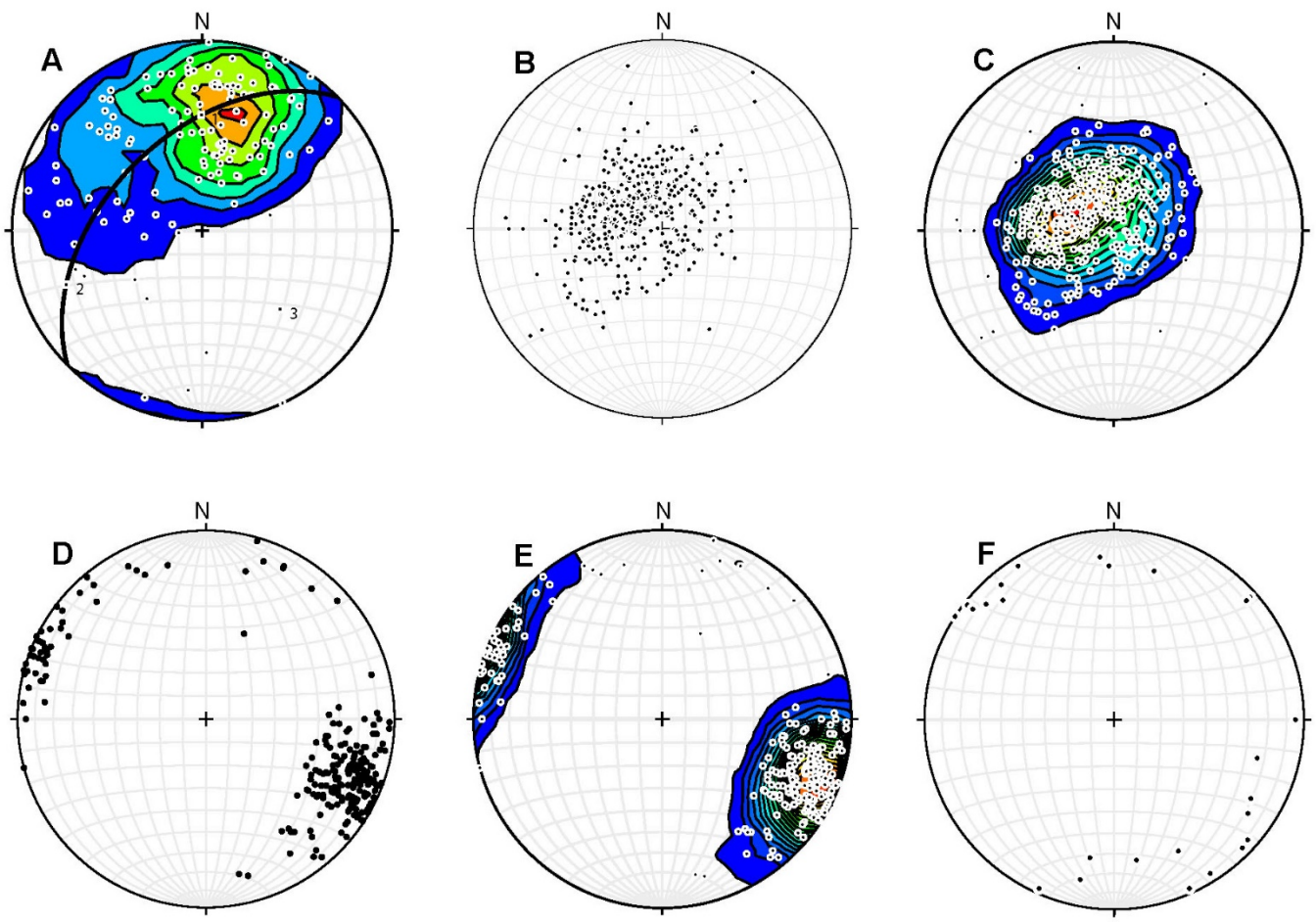

Figure 5. Equal-area, lower hemisphere projections of structural data from the Secret Valley quadrangle. Kamb contours are at intervals of 2σ for all plots. A. Bedding (filled black circles, N = 125) in sedimentary rocks (Ŧt–ℙMdp) above the Ruby Mountains–East Humboldt Range detachment fault. The pole to a best-fit great circle indicates an average fold axis of 41º/135º. The poles to bedding are contoured by the Kamb technique. B. Foliations (filled black circles, N = 424) in metasedimentary and deformed intrusive igneous rocks of the metamorphic and igneous complex. C. Poles to foliation contoured by the Kamb technique. D. Elongation (stretching) lineations (filled black circles, N = 238) in metasedimentary and deformed intrusive igneous rocks of the metamorphic and igneous complex. The scatter of some of the data is interpreted as elongation lineations rotated by superposed Tertiary post-mylonization folds or lineations associated with the hinge zones of the superposed folds. E. Lineations contoured by the Kamb technique; F. Hinge lines of folds in the metamorphic and igneous complex (N = 25).

the strata chiefly dip to the southeast to south. The sedimentary rocks are broken into various fault blocks so well-defined folding is not apparent on the geologic map. In figures 5B and C, poles to metamorphic foliation are shown indicating a 'bull's eye' pattern dominated by low to moderate dips. Steep dips are not common in the map area in the metamorphic and igneous complex. The measured foliations in the Secret Valley quadrangle are chiefly part of the Tertiary mylonitic shear zone, and an associated elongation (stretching) lineation (figs. 5D, E) occurs on the foliation plane. The trend of the lineation is dominantly WNW–ESE with some scattered lineations to the NW–SE. Lineations that plot away from this pattern are interpreted as lineations that have been rotated during post-mylonitic folding. Radiometric dating and thermochronology dates the penetrative fabric of the mylonitic shear zone as over by ~29–23 Ma (Dokka et al., 1986; Wright and Snoke, 1993). The mylonitic fabric locally is deformed by post-mylonitic plastic folding (figs. 4A, B). Metamorphic foliation in the Sharps Creek area and north (Snoke, 1980; fig. 5F) where mylonitic fabrics are not well developed (fig. 6) is folded by northwest-trending folds with southwestern vergence; the foliation and folds may indicate pre-mylonite deformation that could represent a Mesozoic history (Late Cretaceous?).

Disconnected lenses of marble and calc-silicate rock (Zmm) interpreted to correlate to Unit G of the Neoproterozoic McCoy Creek Group are interleaved with quartzite and schist (ЄZpmi) in upper-amphibolite facies footwall rocks in the southwestern part of the quadrangle. We interpret these lenticular bodies as structurally dismembered by cryptic structures during metamorphism before and during mylonitization.

In summary, the crystal-plastic deformational history in the Secret Valley quadrangle and environs can be divided into four successive phases of deformation: (1) possible Mesozoic fabrics (foliation and folds) and older-on-younger faulting that pre-dated mylonitization, (2) a pervasive mylonitic shear-zone deformation of mid-Tertiary age (~29–23 Ma), (3) late metamorphic, post-mylonitic folding with westward vergence, and (4) plastic-to-brittle low-angle normal faulting that defines the RM-EHR detachment-fault zone and predates middle Miocene rocks including 15-Ma rhyolite. Phases 2, 3, and 4 may constitute a continuum in progressive extensional deformation. Initiation of younger normal faulting that helped block out the modern basin-and-range topography predates an alluvial unit assigned an age of Pleistocene to Pliocene(?).

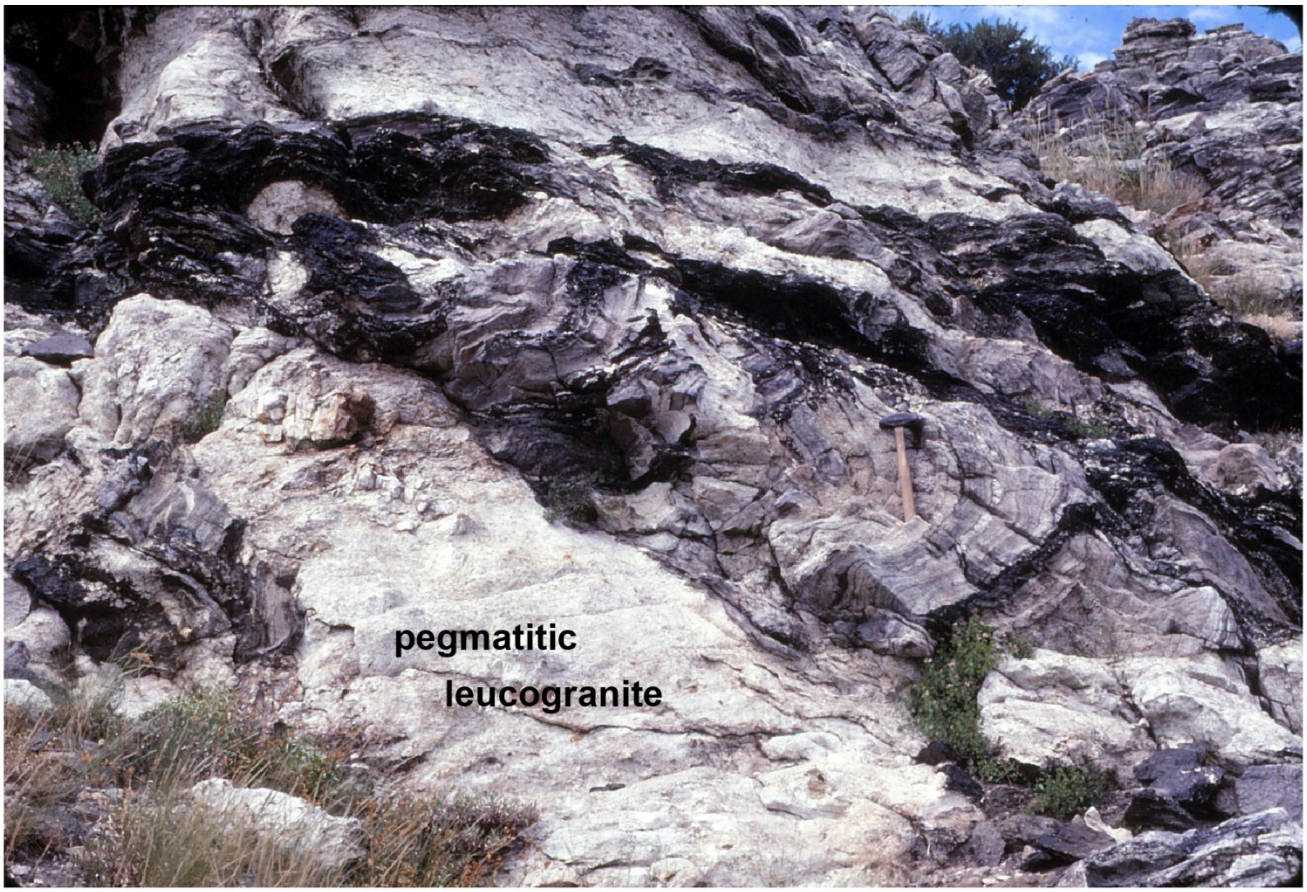

Figure 6. Locality in the ЄZpmi unit exposed on the northeastern flank of the northern Ruby Mountains where a sample was collected for U-Pb-Th monazite dating (see U-Pb monazite locality 1 on the geologic map). The monazite occurs in biotite schist (dark layer in the upper part of the photograph), which is intercalated with migmatitic biotite feldspathic metaquartzite and intruded by pegmatitic leucogranite (TKlg). Some of the pegmatitic leucogranite is post kinematic and cuts across the folded structure. A hinge line of a fold at this locality is 8º/320º and axial surface is 283º, 14º. An axial surface foliation is associated with the hinge zone of the fold.

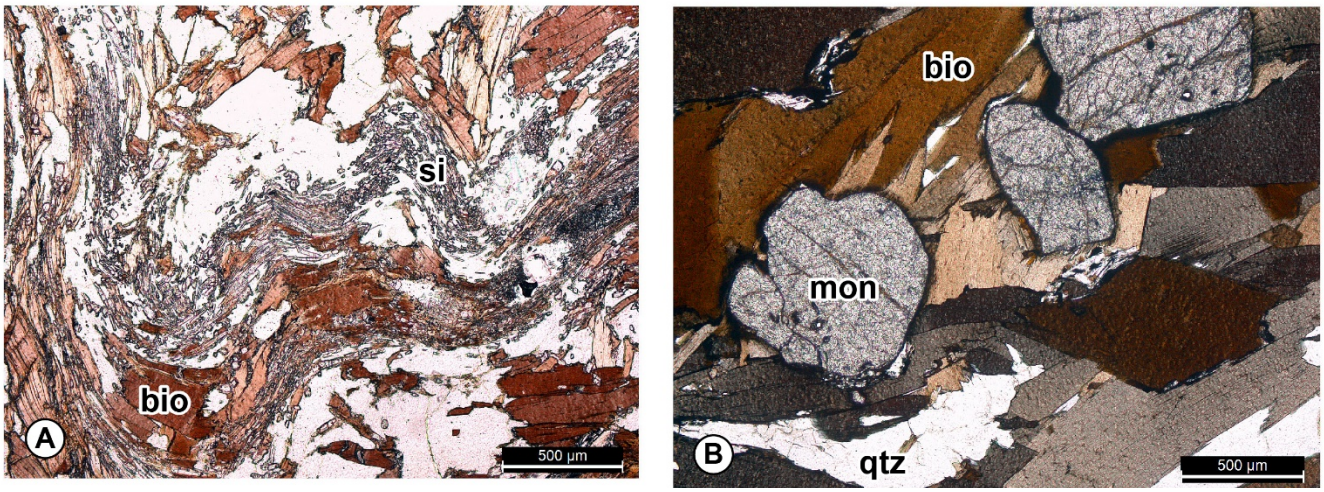

Figure 7. Photomicrographs of schists from the ЄZpmi unit. A. Folded quartz + biotite + sillimanite + plagioclase + muscovite + garnet (not in the field of view) schist (PPL); bio = biotite, si = sillimanite. The epitaxial growth of sillimanite on biotite is characteristic in this metapelitic schist. Note that sillimanite prisms are folded by post-metamorphic folds. B. Monazite-biotite schist (PPL); mon = monazite, bio = biotite, qtz = quartz. Pb-U-Th monazite ages from this sample indicate Late Cretaceous metamorphism. See U-Pb monazite locality 1 on the geologic map.

Seismic-reflection profiling was carried out in the Secret Valley quadrangle (Valasek et al., 1989). The route of the seismic-reflection profile began on the east where the Franklin River crosses the North Ruby Valley Road (county road 786) and went westward to the intersection with Nevada 229. Then the route trended to the northwest along Nevada 229 to virtually the western boundary of the Secret Valley quadrangle (see Valasek et al., 1989, their plate 1). The highly reflective character of the seismic profile is interpreted as the constructive interference of the planar nature of the layering, compositional heterogeneity, and anisotropy in the mylonitic shear zone (Valasek et al., 1989). East- and west-dipping reflectors in the seismic section correlate with exposed, opposing dipping mylonitic foliation domains in the Secret Valley and Tent Mountain (Hurlow, 1987) quadrangles supporting the concept that the mylonitic shear zone was tilted or warped during tectonic exhumation. Valasek et al. (1989) also suggested that opposing dip domains could be a product of the anastomosing character of shear zones during progressive inhomogeneous simple shear. An alternative model is that the northern Ruby Mountains and southwestern East Humboldt Range are an example of a double dome structure that has been documented in some core complexes (e.g., Naxos dome, Greece; Rey et al., 2011). However, a medial high-strain zone expected for a double dome structure (Rey et al., 2011) is not recognized in the surface geology of the RM-EHR core complex or the seismic-reflection profile. The opposing dipping mylonitic foliation domains in the Secret Valley and Tent Mountain quadrangles form a unique aspect that has not been documented in any other part of the RM-EHR core complex. Its origin could be fundamental to the development of this core complex.

High-angle normal faults are common in the Secret Valley quadrangle. The late Cenozoic range-front fault system bounding the eastern flank of the Ruby Mountains is exposed west of Secret Pass as the steeply dipping Poison Canyon normal fault (see cross section A–A'). The Poison Canyon fault juxtaposes Permian to Pennsylvanian rocks against the ЄZpmi unit of the metamorphic and igneous complex (see cross section A–A'). This normal fault is interpreted as a major frontal fault related to the range-front fault system. The Poison Canyon fault is estimated to have approximately one km of total displacement along it. In the vicinity of Secret and Gardner creeks, fault scarps up to 4 m high are present along the Poison Canyon fault in alluvial fan deposits of likely middle Pleistocene age (Qfo). The fault continues northward in bedrock into the Tent Mountain quadrangle where it gradually loses displacement (Hurlow, 1987). To the south adjacent to Ruby Valley the fault is buried under Quaternary deposits (Qfo) and is part of the eastern frontal fault system of the Ruby Mountains. This fault truncates the RM-EHR detachment fault, which emplaced Lower Triassic to Pennsylvanian units onto the metamorphic-igneous footwall. In the 'Secret Hills' another N–S-striking fault is part of the range-front system (see cross section A–A'). At this locality, a normal fault downdrops undivided Lower Permian rocks of the hanging wall adjacent to metamorphic rocks on the footwall. This normal fault also truncates the RM-EHR detachment fault, which places undivided Lower Permian rocks onto metamorphic rocks of the footwall. This range-front fault system post-dates the middle Miocene Humboldt Formation.

CONDITIONS OF METAMORPHISM

Metamorphism in the metamorphic rocks in the Secret Valley quadrangle ranges from upper-amphibolite facies (sillimanite-muscovite zone) to greenschist facies. The highest-grade rocks contain the assemblage: quartz + biotite + sillimanite + plagioclase + muscovite + garnet + apatite + zircon, which occurs in metapelitic schist (fig. 7A) of the Neoproterozoic McCoy Creek Group within the ЄZpmi map unit. Two schists in this unit from the southwestern corner

of the Secret Valley quadrangle contain assemblages that indicated P–T conditions of ~4 kb and 600 ºC (Hodges et al., 1992). These rocks are migmatitic with layers of leucosome varying meter- to centimeter-scale (fig. 8). Calc-silicate-bearing quartzite, also in the Neoproterozoic McCoy Creek Group (€Zpmi unit), contains the subassemblage of hornblende + diopside + garnet suggesting an original protolith of ferruginous dolomitic sandstone. Lenses of coarse-grained, white graphitic calcite marble and calc-silicate rock (Zmm) are interpreted as dismembered layers of metacarbonate rocks in the Neoproterozoic McCoy Creek Group [(Unit G) of Misch and Hazard (1962), Woodward (1967), and Miller (1983)].

The O€mi unit contains a variety of impure calcite marble and calc-silicate paragneiss. Typical impurities in the calcite marble are graphite and muscovite. Some marble contains dolomite. The calc-silicate paragneiss has much more interesting assemblages such as: calcite + quartz + plagioclase + diopside + phlogopitic biotite + scapolite + titanite. This assemblage indicates upper-amphibolite facies conditions.

Figure 8. Mylonitic migmatitic metaquartzite and schist of the €Zpmi unit. Note the lenticular layers of deformed pegmatitic leucogranite (TKlg). The rocks are dipping to eastward (to the right), but sense-of-shear criteria indicate top to the west-northwest (i.e., up the dip of the foliation). The eastward dip of foliation in the mylonitic shear zone is interpreted to indicate the shear zone was tilted or warped during its development (see Spencer, 1984).

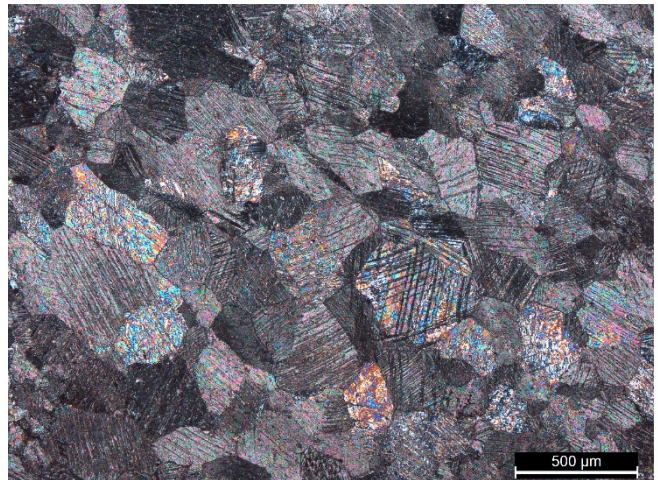

Figure 9. Photomicrograph of recrystallized meta-limestone of the Pennsylvanian Ely Limestone (crossed polars [XP]). Note the granoblastic texture and deformation twinning in calcite of this meta-limestone. These textural characteristics and conodont CAIs of 5–6 indicate that the Ely Limestone was locally heated by hydrothermal fluids related to juxtaposition against the hot footwall of the metamorphic and igneous complex below the RM-EHR detachment fault.

Conodont alteration indices (CAIs) provide a measure of the estimate temperature reached in low-grade marbles and limestones (Epstein et al., 1974; Rejebian et al., 1987). Samples of metamorphosed Lehman Formation (Middle Ordovician) contain diagnostic conodonts which yielded CAIs of 5 (locality C13) and 5–6 (C14), indicating that the host rock reached 300–400 ºC. Samples from the Ely Limestone (localities C7 and C8) also yielded CAIs of 5–6 indicating the host rock reached 300–400 ºC. This Pennsylvanian meta-limestone is recrystallized to a low-grade marble (fig. 9) with lenticular meta-chert. Similar low-grade Ely Limestone also occurs in the Gordon Creek quadrangle (Sicard and Snoke, 2020). An unusually high CAI of 7 was reported by Anita G. Harris (U.S. Geological Survey, written commun., 1983) from the Pequop Formation at locality C4, indicating host rock temperature reached about 450 ºC. These high CAIs for rocks in the hanging wall of the RM-EHR detachment fault may indicate that they locally were metamorphosed during the juxtaposition of a hot footwall terrane adjacent to these limestone units. These elevated CAIs are interpreted to be related to hot fluids generated from the metamorphic and igneous footwall of the detachment-fault system.

DESCRIPTION OF MAP UNITS

Quaternary Surficial Deposits

Qfy Youngest alluvial-fan deposits (Holocene) Deposits of silt, sand and pebble- to cobble- sized gravel in active to and recently abandoned alluvial fans and active ephemeral stream channels. Includes subrounded to subangular clasts of primarily mylonitic quartzite, gneiss, and granitic rocks derived from the adjacent ranges. Surfaces locally have subtle bar and swale morphology near fan heads and within

active channels, otherwise planar to mildly dissected by gully erosion. Inset below adjacent Qfi and Qfo deposits. Thickness is up to ~5 m.

Qls Landslide deposit (Holocene to late Pleistocene) Slope failure deposits with a wide range of characteristics and compositions. Locally dominated by highly fractured or jumbled bedrock, with a varying percentage of poorly to moderately sorted gravels and fines. Typically form uneven, hummocky surfaces. Head scarps vary from sharp and fresh to rounded and indistinct. Qls deposits are common adjacent to Devils Slide Canyon and in the upper catchment of Secret Creek on the east flank of the northern Ruby Mountains. These landslides likely resulted from rapid incision of Secret Valley following integration with the Humboldt River catchment. Estimated thickness is up to ~15 m.

Qc Colluvium (Holocene) Unconsolidated, angular to slightly rounded boulders to pebbles of bedrock in a variably sandy matrix. Commonly 1–5 m thick.

Qfi Intermediate-aged alluvial-fan deposits (late Pleistocene) Coarse-grained alluvial deposits in mostly inactive alluvial fans and channels; typically sandy pebble- to cobble-sized gravel, and boulders. Subrounded to subangular clasts of primarily mylonitic quartzite, gneiss, and granitic rocks derived from the adjacent ranges. Surface morphology is generally planar with rounded margins. On the east flank of the northern Ruby Mountains Qfi fans commonly bury Qfo surfaces near the range-front, but downslope become confined to inset channels in the Qfo surfaces. Drainages incised into Qfi have a tributary pattern with channel incision ranging from 1–3 m. Soils consist of stage I–II $CaCO_3$ horizons (Bk) up to 1 m thick. Thickness is up to ~10 m.

Qfo Older alluvial-fan deposits (middle Pleistocene?) Coarse-grained alluvial deposits in inactive alluvial fans; typically sandy pebble- to cobble-sized gravel with boulders. Subrounded to subangular clasts of primarily mylonitic quartzite, gneiss, and granitic rocks derived from the adjacent ranges. Surface morphology ranges from planar to fully rounded erosional remnants. Locally mantled by an eolian cap. Surfaces are dissected with incised channels up to 7 m deep. Stage II–III $CaCO_3$ horizons up to 2 m thick that locally form a semi-continuous carbonate rich layer. Qfo surfaces are abandoned on the south side of Devils Slide Canyon, with the active Secret Creek channel incised over 60 m below. These deposits contain cobble- to boulder-sized clasts of rhyolite (Tr) sourced from outcrops only present on the north side of Secret Creek and suggests incision of Devils Slide Canyon post-dates deposition of Qfo. This relationship also suggests that Qfo deposits in the upper Secret Valley catchment were deposited into an internally drained basin that predates the integration of Secret Valley into the upper Humboldt River catchment. Qfo in the vicinity of Secret and Gardner Creeks is faulted by the Poison Canyon fault with scarp heights of approximately 3–4 m. Maximum thickness is estimated at ~30 m.

Qgm Glacial moraine deposits (Pleistocene) Deposits of poorly sorted sand, gravel, and boulders forming moraines. Moraines may be from the Angel Lake and/or Lamoille glaciations (Sharp, 1938, Wayne, 1984; Laabs et al., 2020). Includes subangular to subrounded clasts of mylonitic quartzite, gneiss, and granitic rocks.

Qgo Glacial outwash deposits (Pleistocene) Deposits of silt, sand, and pebble-to cobble-sized gravel with boulders up to 3 m in diameter. Includes rounded to subrounded clasts of mylonitic quartzite, gneiss, and granitic rocks. Higher percentage of boulders than nearby alluvial-fan deposits. Alluvial outwash from Angel Lake and/or Lamoille glaciation in the upper Franklin River catchment. (Sharp, 1938, Wayne, 1984; Laabs et al., 2020).

QToa Oldest alluvium (early Pleistocene to Pliocene?) Coarse-grained alluvial deposits; typically sandy pebble- to cobble-sized gravel with abundant boulders. Clasts are subrounded to subangular. Surfaces are fully rounded erosional remnants perched up to 30 m above active stream channels. Soil horizons are entirely stripped. Maximum thickness is estimated at ~50 m.

Tertiary Volcanic and Sedimentary Rocks

Tj Jasperoid breccia (Pliocene to Miocene) Massive siliceous breccia commonly re-cemented by quartz, associated with normal-sense fault zones (either high- or low-angle), commonly black to dark or medium gray on a fresh surface; a rusty red patina is characteristic of some outcrops. This unit also includes cream-colored to white siliceous breccia and vuggy siliceous veins. All these siliceous rock types are interpreted as the result of hydrothermal replacement of an original host rock.

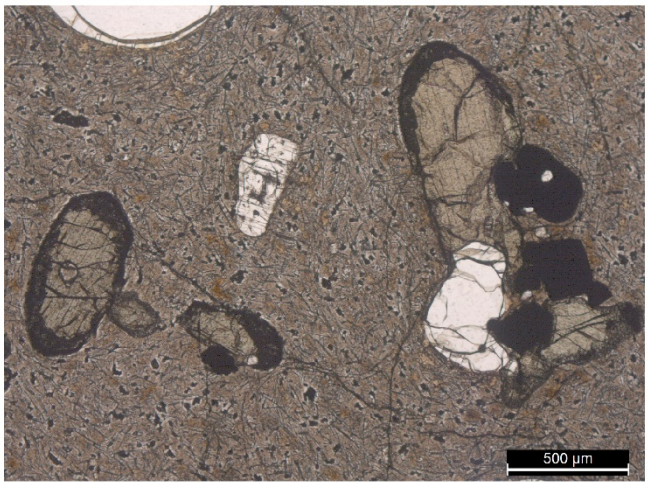

Figure 10. Photomicrograph of clinopyroxene-bearing rhyolite vitrophyre (PPL). The clinopyroxene is green suggesting a hedenbergitic component. Sanidine from this rock yielded a K-Ar date of 15 ± 1.5 Ma. See locality 'A' on the geologic map.

Tr Rhyolite (Miocene) Brown-red- to orange-red-weathering, porphyritic rhyolite flows and flow breccias with small phenocrysts (1–2 mm) of sanidine and quartz. Samples are typically vuggy and partially silicified. Scarce black vitrophyre at the base of some flows. The vitrophyre commonly contains green hedenbergitic pyroxene (fig. 10). New dating of a rhyolite flow in the northwestern part of the quadrangle yielded a $^{40}Ar/^{39}Ar$ anorthoclase age of 15.37±0.04 Ma for Tr (H14-54; table 1) (Chris Henry, personal commun., 2020). Sanidine from a vitrophyre yielded a K-Ar date of 15.0 ± 1.5 Ma (E.H. McKee, written commun., 1978; reported in Snoke, 1980) (K-Ar sample locality A; table 1). The rhyolite is associated with the Humboldt Formation and correlated with the middle Miocene Willow rhyolite suite in the Welcome quadrangle (McGrew and Snoke, 2015).

Th Humboldt Formation (Miocene, ~16–10 Ma after Colgan et al., 2010) Pale green conglomerate, sandstone, siltstone, and accretionary lapilli tuff. Sandstone and siltstone are tuffaceous. Clasts in conglomerate and sandstone beds are chiefly derived from Pennsylvanian–Mississippian Diamond Peak Formation and reworked Tertiary sedimentary and volcanic rocks of the Humboldt Formation. Detrital biotite visible in hand sample in sandstone beds exposed in Secret Valley. In the Soldier Peak and Heelfly Creek quadrangles, the conglomerates contain scarce deformed metaigneous and metasedimentary clasts (mylonitic leucogranite orthogneiss, mylonitic Eureka Quartzite, and calcite marble) derived from the subjacent metamorphic and igneous complex exposed in the Secret Valley quadrangle and environs (Snoke, 1980; Dee et al., 2015). In Snoke (1980) and Snoke and Howard (1984), the Humboldt Formation in the Secret Creek gorge area was interpreted as part of the detachment-fault system. More recent mapping by Dee et al. (2015) indicate that the Humboldt Formation is unconformably deposited on Paleozoic sedimentary rocks as well as rocks of the metamorphic and igneous complex. Therefore, the previous interpretation of a fault boundary at the base of the Humboldt Formation is obsolete.

Tvs Volcanic and volcaniclastic rocks (middle Eocene) Andesitic lava flows, flow breccias, volcaniclastic rocks, and volcanogenic epiclastic rocks. Propylitic alteration is common in these intermediate volcanic rocks. Brooks et al. (1995) reported three $^{40}Ar/^{39}Ar$ dates from similar andesitic rocks collected at the southern end of the East Humboldt Range. These ages and the minerals dated are: 38.8 ± 0.4 Ma (hornblende, their sample 91T12), 39.5 ± 0.3 Ma (hornblende, their sample 91T17), and 40.98 ± 0.1 Ma (biotite, their sample 91T19).

Unmetamorphosed Sedimentary Rocks

Ŧt Thaynes Formation (Early Triassic) Gray to chocolate brown, thick-bedded to laminated limestone, bioclastic limestone, siltstone, sandstone, and dolomite. The Thaynes Formation is separated from the underlying Park City Group (Ppc) by a regional unconformity (Collinson et al., 1976).

Ppc Park City Group, undivided (Late Permian) Light-gray to white limestone with white nodular chert, light-gray dolomite with white nodular chert, bedded chert, phosphatic shale, siltstone, and fine-grained sandstone. This undivided unit is interpreted as a composite of the Kaibab Limestone, Plympton Formation, and Gerster Limestone, which compose the Park City Group in northeastern Nevada (Wardlaw and Collinson, 1978). These units are well-exposed and subdivided in the southeastern East Humboldt Range (Taylor, 1984).

Pu Permian sedimentary rocks, undivided (Early Permian) Limestone, cherty limestone, fine-grained sandstone, and scarce conglomerate. This undivided unit is interpreted as a composite of the limestone and conglomerate unit (Plc) and Pequop Formation (Pp); see below for detailed rock descriptions. From a silty limestone sample collected at megafossil/fusulinid locality 1 containing scattered crinoid columnals and fusulinids, Raymond C. Douglass (U.S. Geological Survey, written commun., 1973) identified a staffelid and Schwagerina sp. of probable Leonardian age but possibly late Wolfcampian. This fauna is typical of either the Riepe Spring Limestone or Ferguson Mountain Formation (Berge, 1960).

Pp Pequop Formation (Early Permian) Purplish-gray, platy (slope-forming) silty limestone and massive- to thick-bedded, medium- to dark-gray, fine-grained limestone; locally fusulinid-rich coquina; yellow-weathering, calcareous fine-grained sandstone; a laterally continuous, resistant chert-clast conglomerate (2–5-m thick) forms the top of the formation. From a silty limestone with abundant fusulinids collected at megafossil/fusulinid locality 2, Douglass identified large specimens of Parafusiulina sp. of early Leonardian age. This fauna is typical of the Pequop Formation. From silty limestone samples collected at megafossil/fusulinid locality 3, Raymond C. Douglass (U.S. Geological Survey, written commun., 1972) identified the following fusulinds: Schwagerina sp., Parafusulina sp. (small form), Schubertella sp., Textularid, and Endothyrid. This fauna is indicative of the lower part of the Pequop Formation (Leonardian in age). A limestone sample from locality C1 yielded conodont remains of Hindeodus sp. and Neostreptognathodus ruzhencevi Kozur, which indicate an age of late early Leonardian (Anita G. Harris, U.S. Geological Survey, written commun., 1983). The determined CAI is 2–4, indicating a temperature range of 90–200 ºC. A similar late early Leonardian conodont fauna was identified at localities C2 and C3, with CAIs of 1–1 ½ and 2, respectively. Conodont remains from locality C4 yielded an age of late early to early late Leonardian, but an anomalously high CAI of 7, indicating that the host rock reached about 450 ºC (Anita G. Harris, U.S. Geological Survey, written commun., 1983).

Plc Limestone and conglomerate (Early Permian) Massive-bedded, medium-gray to dark-gray cherty limestone, chert is commonly gray to black and forms irregular masses to lenticular layers; also light-gray limestone with yellowish-orange chert masses, some massive limestone beds without chert; locally fusulinid-rich limestone; chert- and limestone-clast, calcareous conglomerate and grit, limestone beds intercalated with conglomeratic strata, chert-clasts in conglomeratic rocks are chiefly light colored (white, pale gray, and yellowish tan). From samples collected at megafossil/fusulinid locality 4, Raymond C. Douglass (U.S. Geological Survey, written commun., 1973) identified abundant large specimens of Monodiexodina sp. in a yellow-tan calcareous sandstone. At the same locality from a dark gray silty to sandy limestone composed chiefly of fusulinids, he identified the small forams Bradyina sp. and Cimacammina sp. and the fusulinids included Schubertella sp., Pseudoschwagerina sp., and Schwagerina sp. From megafossil/fusulinid locality 5, Douglass identified Bradyina sp. and Cimacammina sp. and Schubertella sp., Schwagerina sp., Pseudofusulina(?) sp., and rare Monodiexodina sp. in a sample of sandy limestone containing bryozoans and abundant forams. At the same locality from a sample of calcareous sandstone, he identified Bradyina sp. and Pseudofusulina sp. The fauna from both localities are typical of the Riepe Spring Limestone or Ferguson Mountain Formation (Berge, 1960). C.H. Stevens (1979, p. 450 and his figure 16) reported a zone of Eoparafusulina linearis associated with conglomerate in the lower part of the Lower Permian section exposed near Secret Valley, which suggests a possible correlation with either the Ferguson Mountain Formation or Riepe Spring Limestone. From a limestone sample collected at locality C5, Anita G. Harris (U.S. Geological Survey, written commun., 1984) identified elements of the following conodonts: Adetognathus lautus (Gunnell), Idiognathodus sp., and Streptognathodus Elegantulus Stauffer and Plummer, which indicate an age range from Early Permian–Pennsylvanian (middle Wolfcampian–Morrowan). These conodont remains have a CAI of 4 to 4½, indicating that the host rock reached 200–250 ºC. This locality lies immediately above the RM-EHR detachment fault. From locality C6, Anita G. Harris identified elements of Adetognathus lautus (Gunnell) and Idiognathodus sp. which provide an age range of Early Permian–Pennsylvanian (middle Wolfcampian–Morrowan). The CAI of the conodont remains is 3, indicating that the host rock reached 120–150 ºC. Taken together the fossil assemblage suggests the deposits span the early Leonardian to Wolfcampian series of the Early Permian.

Pe Ely Limestone (Pennsylvanian) Light- to medium-gray resistant thick-bedded limestone with yellowish tan nodular or lenticular chert interlayered with slope-forming, thin-bedded limestones, locally includes bioclastic limestone with brachiopod fauna, crinoid columnals, and other fossil fragments. Metamorphosed Ely Limestone occurs along the northeastern flank of the northern Ruby Mountains and ranges from pale-gray to bluish-gray calcite marble with accessory graphite, creamy yellow calcite marble, and medium-gray calcite marble with lenticular metachert masses. Metamorphosed Ely Limestone displays heterogeneous recrystallization and plastic deformation (fig. 9). A sample from locality C7 yielded a conodont fauna that included: Adetognathus lautus (Gunnell), Idiognathodus Delicatus (Gunnell), Hindeodus sp. indet., Neognathodus medadultimus Merrill, and Neognathodus Medexultimus Merrill, which indicates upper Middle Pennsylvanian age (Desmoinesian). The CAI from this sample is 5–6, indicating that the host rock reached 300–400 ºC (Anita G. Harris, U.S. Geological Survey, written commun., 1983). A sample from locality C8 contains a similar conodont fauna and also has a CAI of 5–6. This heating may relate to juxtaposition of the Ely Limestone onto the hot footwall of the RM-EHR detachment fault. In contrast, conodont remains from limestones collected at localities C9, C10, and C11 yielded Desmoinesian–Atokan age (Middle Pennsylvanian) with a CAI of 3, indicating host rock temperatures only reached 120–150 ºC. Limestone samples from megafossil/fusulinid locality 6 yielded an abundant well-silicified brachiopod fauna of Desmoinesian (Pennsylvanian) age. Bruce Wardlaw (U.S. Geological Survey, written commun., 1976) recognized the following brachiopod species in this sample: Koslowskia sp., Desmoinesia sp., Buxtonia sp., Antiquatonia sp., small Pontisiid Rhynchonellid resembling Acolosia, Cleiothyridina sp., Composita Subtilita (Hall), Hustedia Miseri Gibbosa Lane, Crurithyris Planoconvexa (Shumand), Neospirifer sp., Dielasma sp., and Beecheria sp. Pennsylvanian (Desmoinesian[?]) bryozoan were identified

Figure 11. Sawed slabs of Lower Pennsylvanian–Mississippian Diamond Peak Formation. On the left is undeformed Diamond Peak conglomerate characterized by angular clast chert. On the right is mylonitic Diamond Peak conglomerate located in T. 34 N, R. 60 E., NE quarter of section 13 containing strongly deformed chert clasts. This metaconglomerate is interpreted as a slice of Diamond Peak Formation in the Tertiary mylonitic shear zone. This slice of mylonitic Diamond Peak Formation is structurally above the composite O€mi unit but structurally below klippen of Oe. These structural relations indicate an older-on-younger structural stacking, which is unusual in the Ruby Mountains–East Humboldt detachment-fault zone.

by Olgerts L. Karkins (U.S. Geological Survey) from this unit (see Snoke, 1980, Appendix 1, p. 329–330). The contact with underlying Diamond Peak Formation is gradational.

ℙMdp Diamond Peak Formation (Early Pennsylvanian to Mississippian) Dark yellow to red-weathering, subangular to subrounded chert-clast and quartzite-clast conglomerate and grit, tan-weathering sandstone, black shale, and locally massive medium gray micritic limestone containing sparse irregular chert nodules. From a sample of limestone collected from locality C12, Anita G. Harris (U.S. Geological Survey, written commun., 1984) recovered remains of the conodont Hindeodus scitulus (Hinde), which is a shallow-water species that ranges from late Chesterian into the very latest Osagean, indicating a Late Mississippian age. The determined CAI is 4, indicating that the host rock reached about 200 ºC. In T. 34 N, R. 60 E., NE quarter of section 13, outcrops of mylonitic conglomerate and grit, containing strongly deformed chert clasts (fig. 11), are interpreted as a slice of Diamond Peak Formation in the Tertiary mylonitic shear zone. At UTM coordinates, 4521734 northing, 0656157 easting (Universal Transverse Mercator NAD 1983), the mylonitic foliation and elongation (stretching) lineation in the unit are: 97º, 25º S (s,d) and 13º/127º (p/t), respectively. This attitude is similar to attitudes taken in the mylonitic shear zone throughout the Secret Valley quadrangle. This slice of mylonitic Diamond Peak Formation is structurally above the composite O€mi unit but interpreted as structurally below klippen of metamorphosed Eureka Quartzite (Oe).

Metamorphosed Sedimentary and Deformed Igneous Rocks

Dg Metamorphosed Guilmette Formation (Late Devonian) Gray calcite ± dolomite, color-banded marble, commonly graphitic. Isoclinally folded; locally mylonitic and well foliated.

DOd Dolomitic marble, undivided (Devonian to Ordovician) White to gray, fine- to medium-grained, massive dolomitic marble and scarce lenticular bodies of metasandstone. Compositional layering, where present, typically defined by graphitic-rich laminae; trace tremolite and/or diopside in some samples. Correlated with the Middle Devonian Simonson Dolomite, Lower Devonian Sevy Dolomite, Silurian Laketown Dolomite and Upper Ordovician Fish Haven Dolomite.

Oe Metamorphosed Eureka Quartzite (Ordovician) Massive to mylonitic (foliated and lineated), white vitreous metaquartzite commonly free of impurities except trace amounts of graphite, muscovite, and/or feldspar; gray (graphite-bearing) metaquartzite may be interlayered with the white metaquartzite; scarce calc-silicate-bearing metaquartzite.

Olm Metamorphosed Lehman Formation (Middle Ordovician) Platy, medium-gray meta-limestone with discontinuous yellowish tan silty mottlings (possible deformed burrows); crinoidal debris in some layers. This unit has only been recognized as a tectonic slice in the 'Secret Hills' area (SE quarter of section 23, T. 34 N., R. 60 E.). Middle Ordovician conodonts were recovered by Anita G. Harris (U.S. Geological Survey, written commun., 1984) from meta-limestone samples collected in this unit. From a sample collected at locality C13, Harris identifies 6 elements of Paraprioniodus costatus (Mound), which is a common component of the conodont fauna of the Lehman Formation. The determined CAI is 5, indicating that this meta-limestone reached 250–350 ºC. From another meta-limestone sample collected at locality C14, Harris identified 15 elements of Protopanderous gradatus Serpagli and one element of Paraprioniodus(?) sp. This species association indicates a middle Middle Ordovician age and is consistent with a correlation with the Lehman Formation. The determined CAI is 5–6, indicating the host rock reached 350–400 ºC.

Okq Quartzite of Kanosh Shale (Middle Ordovician) White, vitreous metaquartzite, which resembles Oe. However, this unit is recognized by etching on the surface of rock. This etching is characterized by a pitted surface related to the weathering out of carbonate minerals (probably calcite).

O€m Marble of Verdi Peak, undivided (Ordovician and Cambrian) Light-gray to yellow–tan-weathering micaceous calcite marble and white calcite marble infolded with Oe (SE quarter of section 19, T. 34 N., R. 61 E. and NE quarter of section 30, T. 34 N., R. 61 E.).

O€mi Marble of Verdi Peak, undivided (Ordovician and Cambrian) with deformed igneous intrusions Ordovician to Cambrian metasedimentary rocks intruded by abundant mid-Tertiary quartz dioritic to granitic rocks and Oligocene(?)–Cretaceous coarse-grained to pegmatitic muscovite ± biotite leucogranite (TKlg) (the key characteristics of these intrusive igneous rocks are described below; see Sicard and Snoke [2020] for additional descriptions of these intrusive rock units). Platy gray to white graphite-bearing calcite marble, calc-schist, calc-silicate paragneiss, dolomite-calcite marble, metadolomite, white metaquartzite (possibly quartzite of the Kanosh Shale), pegmatitic Leucogranite (Oligocene[?]–Cretaceous), and locally abundant intrusive mafic (quartz diorite to gabbro) to felsic orthogneiss (early Oligocene to middle Eocene) that form sheet-like to lenticular bodies. Mylonitic textures, including S-C fabric and elongation (stretching) lineation, are common in all rock types except the pegmatitic leucogranite. Although individual intrusive bodies have not been mapped in this unit, the deformed igneous rocks include: quartz diorite of Rattlesnake Canyon, biotite granodiorite–monzogranite orthogneiss of Horse Creek, and muscovite leucogranite orthogneiss of Woods

Creek (see petrographic descriptions and age data below, unit names after Sicard and Snoke, 2020).

ЄZpmi Metamorphosed Prospect Mountain Quartzite (Cambrian and Neoproterozoic protolith age) and McCoy Creek Group quartzite and schist (Neoproterozoic protolith age), undivided and with deformed igneous intrusions Tan- or brown-weathering, medium- to coarse-grained feldspathic micaceous metaquartzite and interlayered pelitic schist and locally calc-silicate quartzite. Commonly migmatitic with pelitic rocks hosting a higher percentage of leucosome than quartzitic layers. The unit locally includes lenticular masses of coarse-grained, white graphitic calcite marble and calc-silicate rock (as in Zmm, see below). Strongly foliated (flaggy) and lineated where in the mylonitic shear zone. Some pelitic schist contains sillimanite and garnet. This unit is intricately intruded by dikes, sills, and irregular masses of pegmatitic leucogranite and lesser amounts of mafic to felsic orthogneiss (see Sicard and Snoke [2020] for detailed descriptions of these rock types in an adjacent quadrangle). A sample of monazite-bearing, biotite schist was collected on the northeastern flank of the northern Ruby Mountains (see U-Pb monazite locality 1 [UTM NAD 1983 coordinates 4516816 northing, 0649075 easting] on the geologic map, also see fig. 6). The monazite grains are readily visible in hand sample with a hand lens (fig. 7B). Snoke et al. (1979) reported Pb-U-Th monazite ages of $^{206}Pb^*/^{238}U$ = 78 Ma, $^{207}Pb^*/^{235}U$= 72 Ma, and $^{208}Pb^*/^{232}Th$ = 1408 Ma, which were interpreted to indicate growth of monazite during Late Cretaceous upper-amphibolite facies metamorphism. Biotite from the same rock yielded a K-Ar age of ~24 Ma (Snoke et al., 1979).

Zmm McCoy Creek Group marble and calc-silicate rock (Neoproterozoic) Coarse-grained, white graphitic calcite marble and calc-silicate rock layers or lenses interlayered with the ЄZpmi unit. Interpreted as original carbonate rock or impure calcareous stratigraphic layers dismembered during deformation and metamorphism. Correlated with metacarbonate rocks in the Neoproterozoic McCoy Creek Group (Unit G) of Misch and Hazzard (1962), Woodward (1967), and Miller (1983). In the Humboldt Peak quadrangle (McGrew, 2018), calcite marble layers yield high $\delta^{13}C$ values, which is interpreted to indicate a Neoproterozoic protolith age (Wickham and Peters, 1993).

Intrusive Rocks

Tgn Mylonitic biotite-muscovite monzogranitic orthogneiss (early Oligocene or middle Eocene?) Description applies to this and to similar but unmapped rocks that occur within the mapped OЄmi and ЄZpmi. Strongly foliated and lineated orthogneiss consisting of perthitic microcline, plagioclase, quartz, muscovite, and biotite with accessory scarce zircon and apatite. This mylonitic orthogneiss is characterized by porphyroclasts in a fine-grained, grain-size reduced matrix. Porphyroclasts of feldspar and muscovite are common. Fractured feldspar porphyroclasts commonly reach 4 mm and exhibit microcracking indicating that mylonization occurred below 450 ºC (Tullis, 1983). Muscovite porphyroclasts are 1 mm or less in size but are visible in hand sample. These lensoidal porphyroclasts exhibit undulatory extinction and commonly indicate sense-of-shear. Very fine-grained, grain-size reduced biotite occurs in wispy anastomosing layers with some larger grains as relicts in the matrix. Quartz occurs as fine-grained, grain-reduced ribbons that exhibit a strong crystallographic orientation. Correlated lithologically with the biotite monzogranite orthogneiss (unit Tmg) in the adjacent Tent Mountain quadrangle, which yielded a U-Pb zircon age of ca. 31.5 Ma (Zuza, et al., 2020; their sample AZ8-19-19(6)).

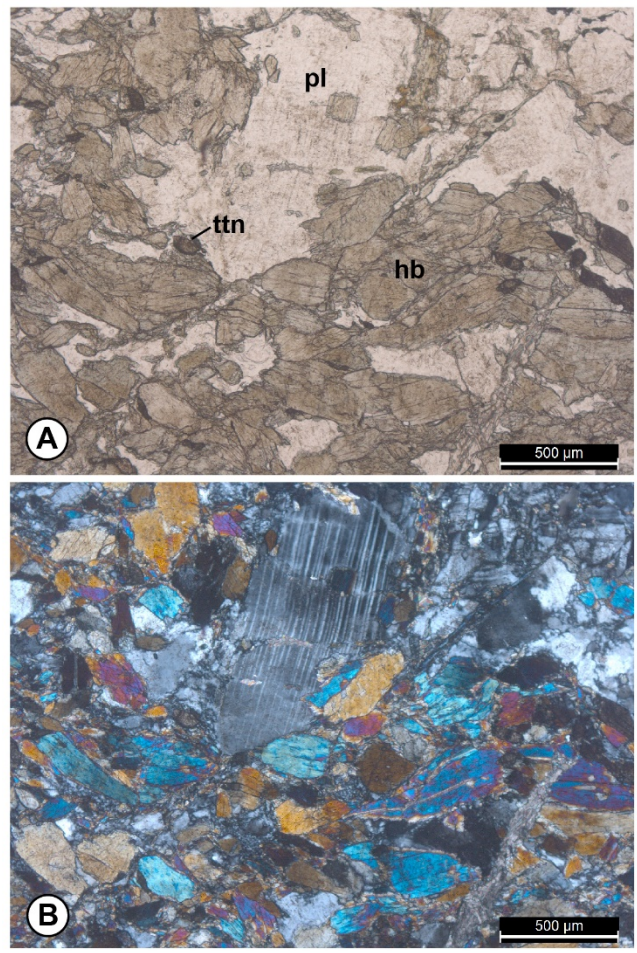

Figure 12. Photomicrographs of middle Eocene(?) quartz-bearing hornblende gabbro from the OЄmi unit. A. Deformed, medium-grained quartz-bearing hornblende gabbro with a relict igneous texture overprinted by grain-size reduction of quartz and plagioclase related to the Tertiary mylonitic shear zone (PPL). Titanite is a common accessory mineral (high-relief, brown mineral). pl = plagioclase, hb = hornblende, ttn = titanite. B. Same view as in A but in XP. Some hornblende grains exhibit undulatory extinction related to deformation.

Tqd Quartz diorite (middle Eocene) (mapped only in one locality, see below); description applies to this rock type and to similar but unmapped rocks that occur commonly within

the O€mi and €Zpmi units. Massive to foliated quartz dioritic rocks consisting chiefly of plagioclase, hornblende, biotite, quartz, and opaque oxides. Accessory minerals include conspicuous titanite as well as epidote-allanite, apatite, and zircon. A relict igneous texture, including zoning of plagioclase grains, is commonly preserved despite weak to moderate deformation. Interstitial quartz patches have undergone partial recrystallization to micro-mosaic aggregates consisting of a mixture of new anhedral grains (neoblasts) and subgrains in older strained grains. Green hornblende grains commonly exhibit a late-magmatic, partial reaction to biotite. Some rocks are meladiorite and hornblende gabbro (fig. 12). These rock types are much subordinate to the quartz dioritic rocks. The ubiquitous presence of both hornblende and biotite suggests that these mafic igneous rocks crystallized from a H_2O-saturated magma. Hornblende is commonly the most abundant mafic mineral in the quartz dioritic rocks, although in some varieties the modal biotite content is greater than hornblende. These mafic rocks typically occur as thin lenticular sheets (<3 m) chiefly within the O€mi and €Zpmi. A small body of this rock type (Tqd) was found within DOd near the center of section 23, T. 34 N, R. 60 E (see geologic map). The quartz dioritic and gabbroic rocks found in the Secret Valley quadrangle are correlated with the middle Eocene quartz diorite of Rattlesnake Canyon (Sicard and Snoke, 2020).

A sample of weakly deformed biotite-hornblende quartz diorite collected from Rattlesnake Canyon in the Gordon Creek quadrangle (Sicard and Snoke, 2020) yielded a U-Pb ID-TIMS zircon crystallization age of ~38 ± 2 Ma (Wright and Snoke, 1993; their RM-13). Farther to the north in the Humboldt Peak quadrangle, a more deformed biotite-hornblende quartz diorite yielded a U-Pb ID-TIMS zircon age of 40 ± 3 Ma (Wright and Snoke, 1993; their sample RM-19; McGrew, 2018). U-Pb zircon dating of unit Tqd in the Tent Mountain quadrangle yielded an age of 39.9 ± 0.2 Ma (Zuza et al., 2020; their sample 060720-4).

TKgs Granitic orthogneiss of Secret Peak (early Oligocene or Cretaceous?) Strongly foliated and lineated two-mica granitic orthogneiss, consisting chiefly of sodic plagioclase, perthitic microcline, and quartz with biotite and muscovite as varietal minerals. Accessory minerals include: myrmekitic intergrowths, zircon, apatite, epidote-allanite, and opaque oxides. Chlorite and sericite are common secondary minerals. Mylonitic texture is characteristic, including local development of S-C fabric, asymmetric feldspar and muscovite porphyroclasts, extensively dynamically recrystallized quartz, grain-size reduction of biotite and replacement by chlorite, and kinking of muscovite. The main mappable intrusion is a sheet-like mass varying in thickness from 50–100-m thick (Soldier Peak quadrangle); numerous thin sheets of similar orthogneiss occur (unmapped) throughout the adjacent €Zpmi unit. Wright and Snoke (1993) reported U-Pb analyses (ID-TIMS method) of four zircon fractions from a sample from this unit (their sample RM-11). All these fractions had extremely high uranium contents. The two coarsest size fractions are nearly concordant at 32 Ma. However, the two <325 mesh-size fractions appear to have suffered extreme post-crystallization radiogenic lead loss. Old $^{207}Pb^*/^{208}Pb^*$ ages of the zircon fractions also suggest an older zircon component. Therefore, the analyzed sample could be significantly older than 32 Ma (e.g., Cretaceous in age).

Jmgp Muscovite granite porphyry (Late Jurassic) Conspicuous muscovite phenocrysts (~3 mm in diameter) with subordinate feldspar microphenocrysts in an aphanitic matrix chiefly consisting of feldspar and quartz. This unit forms a small plug-like mass intruded into unmetamorphosed Ely Limestone. A Rb-Sr muscovite-whole-rock age of 161 ± 2 Ma was determined by Paul D. Fullagar (written commun., 1980; reported in Dallmeyer et al., 1986), whereas muscovite yielded a K-Ar date of 153.9 ± 0.9 Ma (Analyst: E.H. McKee, U.S. Geological Survey; reported in Dallmeyer et al., 1986, their table 2a). The dated sample (197-8) is located in T. 35 N, R. 60 E, SW quarter of section 33 at 115º 12′ 42″ W and 40º 52′ 04″ E (K-Ar sample locality B, see geologic map).

Unmapped Intrusive Rocks

Unmapped intrusive rocks intimately intrude the metamorphic rocks of the footwall (units O€mi and €Zpmi). They include rocks described as the quartz diorite of Rattlesnake Canyon, mylonitic biotite-muscovite monzogranitic orthogneiss (Tgn), and the following rock types. These rock types are mapped and described in the Gordon Creek quadrangle (Sicard and Snoke, 2020)

Muscovite leucogranite orthogneiss of Woods Creek (middle Eocene?) Fine-grained, equigranular muscovite leucogranite orthogneiss. Color index is <5 and locally is hololeucocratic. The chief mineral phases are sodic plagioclase, alkali feldspar, quartz, and muscovite. Accessory minerals include garnet, biotite, apatite, zircon, and opaque oxides. Commonly pervasively foliated and lineated (mylonitic), characterized by dynamic recrystallization of quartz and muscovite. Syntectonic dynamic recrystallization is indicated by grain-boundary migration, subgrain rotation, and the recrystallization of quartz. Asymmetric porphyroclasts of muscovite ('mica fish') (Lister and Snoke, 1984) and domino-type, fragmented feldspar porphyroclasts (Simpson and Schmid, 1983) are also characteristic microstructures in these mylonitic orthogneisses (fig. 13). The rock type occurs as thin lenticular (<3 m) sheets chiefly within the O€mi unit.

Biotite granodiorite–monzogranite orthogneiss of Horse Creek (middle Eocene) Sodic plagioclase, perthitic alkali feldspar, quartz, and biotite are the chief primary minerals. Accessory minerals include muscovite, titanite, zircon, apatite, and opaque oxides. The feldspars constitute about 75% of this medium-grained orthogneiss; fine-grained recrystallized quartz (~15%) and biotite (~7%) occur in

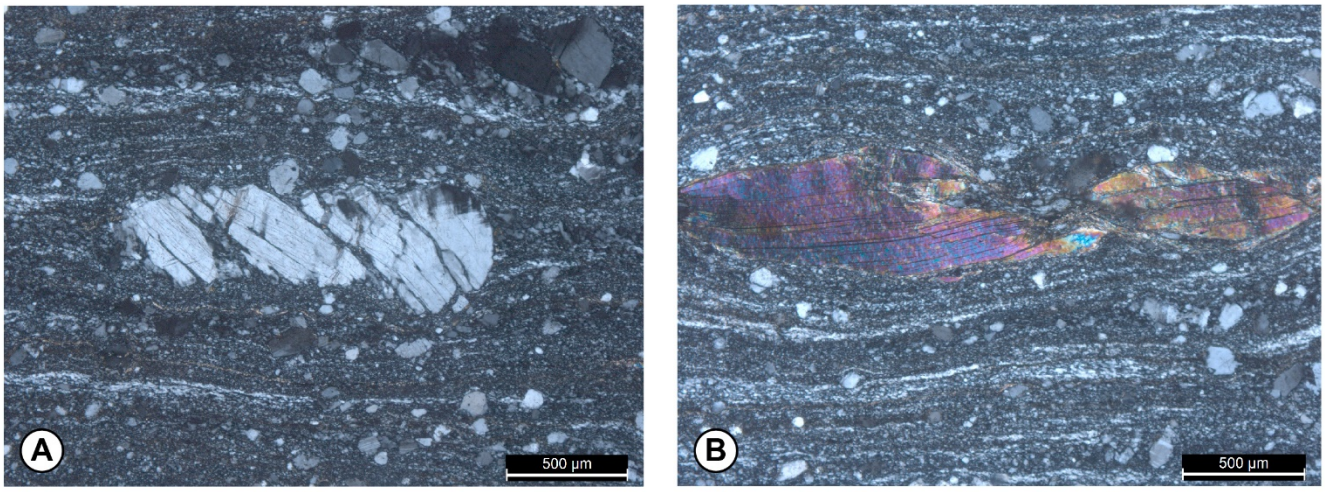

Figure 13. Photomicrographs of sense-of-shear indicators from a mylonitic muscovite leucogranite orthogneiss from the O€mi unit. A. Broken and displaced plagioclase grains in a fine-grained ductile matrix of quartz and feldspar, indicating sinistral shear (XP). The sense-of-shear along the microfractures in the plagioclase grain is opposite to the overall sense-of-shear in the rock (Simpson and Schmid, 1983). B. Muscovite 'fish' in a fine-grained matrix of quartz and feldspar (XP) transected by a microshear that has separated a new 'fish,' which indicates an overall sinistral sense-of-shear in the rock (Lister and Snoke, 1984).

trails around feldspar porphyroclasts. Biotite is locally altered to chlorite (~2%) and muscovite and accessory minerals make up the rest of the rock. Biotite granodiorite–monzogranite orthogneiss is typically strongly foliated and lineated (mylonitic), characterized by extensive syntectonic dynamic recrystallization of quartz and biotite and by porphyroclasts of feldspar. Plagioclase porphyroclast make augen that are chiefly brittlely deformed as indicated by fractured, domino-type grains. Mylonitization is thus near the brittle-to-plastic transition for plagioclase feldspar. Mesoscopic S-C fabric is common in hand specimen. A mylonitic sample of the biotite granodiorite–monzogranite orthogneiss collected from Horse Creek Canyon (Gordon Creek quadrangle) yielded a U-Pb ID-TIMS zircon crystallization age of ~35 ± 3 Ma (Wright and Snoke, 1993; RM-7).

The Horse Creek unit's main lithotype is commonly intruded by pegmatitic granites, which suggests that it overlaps in age with some (Tertiary) leucogranite pegmatite granite. The Horse Creek lithotype occurs as lenticular thin sheets (<3 m) chiefly within the O€mi unit. The rock type lithologically and compositionally (Sicard, 2012) resembles the mid-Tertiary biotite monzogranite in the adjacent Gordon Creek quadrangle (Sicard and Snoke, 2020), which overlaps compositionally (Sicard, 2012), but has larger grain size and presence of feldspar augen (porphyroclasts).

Pegmatitic leucogranite (early Oligocene? to Cretaceous) Leucocratic muscovite ± biotite granite. Typical accessory minerals are garnet and monazite. Monazite from a garnet-muscovite leucogranite, located about 1.3 km southwest of Jerry Crab Spring area (Wright and Snoke, 1993; RM-12, see their table 5; Sicard and Snoke, 2020), yielded a U-Pb ID-TIMS age of ~84 Ma. A syntectonic leucogranite collected from the hinge zone of the Winchell Lake fold-nappe in the northern East Humboldt Range ~20 km north of the quadrangle yielded a U-Pb ID-TIMS zircon crystallization age of 84.8 ± 2.8 Ma (McGrew et al., 2000). SHRIMP dating of zircon from pegmatitic leucogranite from the northern Ruby Mountains about 15 km southwest of the quadrangle yielded a broad spectrum of ages that range from 98 to 26 Ma, with peaks at 92, 68, 42, 37, and 29 Ma (Howard et al., 2011). As noted by Howard et al. (2011) the crystallization and emplacement history of the TKlg is commonly unclear and complicated by the chance that some zircon grains are likely inherited, or the history could have included metamorphic overprinting.

The pegmatitic leucogranite is a very leucocratic rock (color index typically <5) with a heterogeneous coarse texture consisting of alkali feldspar, sodic plagioclase, quartz, muscovite ± biotite, and trace garnet. This coarse-grained granitic rock typically does not exhibit a strong foliation unless it has been deformed in a high-strain zone (fig. 8).

CONCLUSIONS

The Secret Valley quadrangle exposes a long stratigraphic record that ranges from the Quaternary to Neoproterozoic as well as a complex structural history. The following highlights are the fundamental conclusions derived from the geologic mapping of the Secret Valley quadrangle.

1. The map area exposes a cross section through the RM-EHR normal-sense detachment-fault system and related crystal-plastic, mylonitic shear zone. The hanging wall of the brittle, low-angle, detachment-fault zone chiefly contains unmetamorphosed rocks ranging from Lower Triassic Thaynes Formation (Ŧt) to Pennsylvanian–Mississippian Diamond Peak Formation (ℙMdp). In the northwesternmost corner of the quadrangle, this fault zone is overlain by the middle Miocene Humboldt Formation (Th) and associated 15-Ma rhyolite (Tr). These relationships suggest that the brittle history of the RM-EHR detachment-

fault zone pre-dated the middle Miocene (>15 Ma). The age of the brittle detachment-fault zone is inferred to be middle Miocene (17–15 Ma) based on it cutting the mylonitic shear zone (see below) and the truncation by a low-angle normal fault of a 17-Ma basalt dike in the Tent Mountain quadrangle.

2. Metamorphic and igneous footwall rocks to the detachment-fault system are in a mylonitic shear zone in which crystal-plastic deformation ended by 29–23 Ma (late Oligocene) based on K-Ar, fission-track, $^{40}Ar/^{39}Ar$ cooling ages (Kistler et al. 1981; Dokka et al., 1986; and Dallmeyer et al., 1986, respectively) as well as U-Pb (zircon) radiometric dating (Wright and Snoke, 1993). We interpret the Miocene brittle detachment faulting as the youngest and shallowest manifestation of a long-lived extensional shear zone that earlier had mylonitized the deeper and hotter structural levels (Snoke, 1980; Snoke et al., 1997, Snoke, 1998). Retrogression of mylonitic orthogneisses beneath the detachment fault indicate that displacement along the fault post-dated the late Oligocene.

3. Tectonic slices of metamorphosed Upper Devonian (Dg) through Middle Ordovician (Olm) strata are part of the detachment-fault system. Typically, these tectonic slices are arranged with younger rocks structurally above older rocks. However, older-over-younger relations mapped in the Secret Valley and Tent Mountain quadrangles imply structural duplication before the rocks underwent extensional detachment faulting.

4. Sense-of-shear criteria in mylonitic rocks indicate west-northwest shear within the Tertiary shear zone. These data indicate the mylonitic shear zone is west-rooted. Grain-boundary migration, subgrain rotation, and recrystallization of quartz indicate syntectonic dynamic recrystallization. In the Secret Creek gorge area, mylonitic foliation in the €Zpmi unit commonly dips eastward and is truncated by the detachment fault, from which we infer that the mylonitic shear zone tilted or warped before final brittle detachment faulting.

5. Metamorphic footwall rocks in the Secret Valley quadrangle record conditions varying from upper-amphibolite facies (€Zpmi and O€mi) units to greenschist-facies (Olm). Elevated CAIs (5–6) of conodont remains from several meta-limestone samples of the Ely Limestone in the hanging wall of the detachment-fault zone indicate they reached 300–400 ºC. This is interpreted to suggest the Ely Limestone was heated by hydrothermal fluids related to juxtaposition against the hot footwall of the metamorphic and igneous complex.

6. Thermobarometric data and U-Pb monazite dating suggest that the deeper part of the metamorphic and igneous complex reached sillimanite-muscovite zone (upper-amphibolite facies) metamorphism in the Late Cretaceous. Polyphase folding was synchronous with this metamorphism.

7. Intrusive igneous rocks are very common in the €Zpmi and O€mi units. Pegmatitic leucogranite sheets, widespread in these units, range in thickness from centimeters to meters. The age of the pegmatitic leucogranite is interpreted to range from Late Cretaceous to Oligocene based on other studies in the RM-EHR core complex (Lee et al., 2003; Howard et al. 2011; McGrew and Snoke, 2015; McGrew, 2018, Sicard and Snoke, 2020). An extended compositional suite of mafic to felsic deformed intrusive rocks is also an important component of the €Zpmi and O€mi units. U-Pb (zircon) geochronologic data indicate the deformed mafic to felsic intrusive suite was emplaced during the middle Eocene (Wright and Snoke, 1993) and support the concept that the development of the mylonitic shear zone that deformed them was a Tertiary phenomenon related to the unroofing of the metamorphic and igneous complex.

8. Limited exposures of the middle Miocene Humboldt Formation and associated ~15-Ma rhyolite in the quadrangle are interpreted as unconformably deposited on the subjacent unmetamorphosed and metamorphosed rocks, consistent with geologic mapping in the adjacent Heelfly Creek quadrangle (Dee et al., 2015).

9. Late Cenozoic normal faulting produced Basin-and-Range structure, most prominently an east-dipping range-front fault system along the eastern flank of the Ruby Mountains. The system includes the Poison Canyon fault, which is interpreted as an en echelon continuation of the range-front fault system. This east-dipping normal fault cuts the detachment fault and gradually loses displacement to the north in the Tent Mountain quadrangle. The Poison Canyon fault displaces fan deposits of likely middle Pleistocene age (Qfo) with scarp heights of approximately 3–4 m.

10. Secret Valley was integrated into the Humboldt River basin through headward erosion of Secret Creek sometime after deposition of the Qfo fan deposits. This relatively recent integration of the valley was accompanied by incision in the upper reaches of the catchment triggering numerous large landslide complexes.

ACKNOWLEDGMENTS

The initial mapping in the Secret Valley quadrangle occurred between 1971–1973 when Snoke was a National Research Council-U.S. Geological Survey Research Associate at the U. S. Geological Survey, Menlo Park, California. The U.S. Geological Survey provided stipend and field and technical support as well as an exciting atmosphere for geological discussion. M.D. Crittenden, Jr. and K.A. Howard introduced Snoke to the geology of northeast Nevada. Subsequent studies occurred during 1977, 1979–1983, and 1985–1986. Additional Quaternary mapping of the quadrangle occurred in October 2020. Part of this research was funded by the National Science Foundation, Petroleum Research Fund, and USGS National Cooperative Geologic Mapping Program under STATEMAP award number G19AC00383.

Lodging in north Ruby Valley was generously provided by Sim and Dee Duval. Judy, Cindy, and Alison Snoke provided familial companionship and support throughout many years of geologic mapping in the northern Ruby Mountains and East Humboldt Range. Shasta and Sam were

canine companions during the fieldwork. Numerous geologists have provided discussion and insights into the geology of the region, including: Al McGrew, Cal Barnes, Jim Wright, Phyllis Camilleri, Warren Hamilton, Chuck Thorman, Chris Henry, Andrew Zuza, and Tom Anderson. The following paleontologists at the U.S. Geological Survey examined fossil collections and provided valuable stratigraphic age data: Raymond C. Douglass (foraminifera), Bruce Wardlaw (brachiopods), and Olgerts L. Karklins (bryozoan). Also, Anita Harris of the U.S. Geological Survey recovered conodont remains from limestone and meta-limestone samples and provided valuable stratigraphic age determinations (Middle Ordovician–Lower Permian) as well as color alteration indices (CAIs) on many of the samples. We thank Chris Henry for allowing us to use his unpublished $^{40}Ar/^{39}Ar$ age determination on anorthoclase from the Tr unit. We thank Joe Colgan for his helpful review of the penultimate version of the geologic map and text. Finally, the ranchers of north Ruby Valley and Secret Valley are thanked for allowing Snoke to traverse their lands; without their support, much of this work would not have been possible.

We thank Richard Allmendinger for making the Stereonet 11.0.9 software package freely available to us and the entire academic geological community (Allmendinger et al., 2013). Finally, Snoke thanks Phyllis A. Ranz for her expert help on the cartography of the geologic map as well as the preparation of the figures accompanying this report.

The views and conclusions contained in this document are those of the author and should not be interpreted as necessarily representing the official policies, either expressed or implied, of the U.S. Government.

REFERENCES

Allmendinger, R.W., Cardozo, N.C., and Fisher, D., 2013, Structural geology algorithms—vectors and tensors in structural geology: Cambridge, England, Cambridge University Press, 289 p.

Berge, J.S., 1960, Stratigraphy of the Ferguson Mountain area, Elko County, Nevada: Brigham Young University Geology Studies, v. 7, no. 5, p. 1–63.

Brooks, W.E., Thorman, C.H., and Snee, L.W., 1995, The $^{40}Ar/^{39}Ar$ ages and tectonic setting of the middle Eocene northeast Nevada volcanic field: Journal of Geophysical Research, v. 100, p. 10,403–10,416.

Colgan, J.P., Howard, K.A., Fleck, R.J., and Wooden, J.L., 2010, Rapid middle Miocene extension and unroofing of the southern Ruby Mountains, Nevada: Tectonics, v. 29, doi.10.1029/2009TC002655.

Collinson, J.W, St. C. Kendall, C.G., Marcantel, J.B., 1976, Permian-Triassic boundary in eastern Nevada and west-central Utah: Geological Society of America Bulletin, v. 87, p. 821–824.

Dallmeyer, R.D., Snoke, A.W., McKee, E.H., 1986, The Mesozoic-Cenozoic tectonothermal evolution of the Ruby Mountains, East Humboldt Range, Nevada—a Cordilleran metamorphic core complex: Tectonics, v. 5, p. 931–954.

Dee, S., and Ressel, M., 2016, Preliminary geologic map of the Herder Creek quadrangle, Elko County, Nevada: Nevada Bureau of Mines and Geology Open-File Report 16-5, 1:24,000, 5 p.

Dee, S.M., Dering, G.M., and Henry, C.D., 2015, Preliminary geologic map of the Heelfly Creek quadrangle and adjacent parts of the Tent Mountain, Soldier Peak, and Secret Valley quadrangles, Elko County, Nevada: Nevada Bureau of Mines and Geology Open-File Report 15-4, scale: 1:24,000, 5 p.

Dokka, R.K., Mahaffie, M.J., and Snoke, A.W., 1986, Thermochronological evidence of major tectonic denudation associated with detachment faulting, northern Ruby Mountains–East Humboldt Range, Nevada: Tectonics, v. 5, p. 995–1006.

Epstein, A.G., Epstein, J.B., and Harris, L.D., 1974, Conodont color alteration—an index to organic metamorphism: U.S. Geological Survey Professional Paper 995, 27 p.

Hodges, K.V., Snoke, A.W., and Hurlow, H.A., 1992, Thermal evolution of a portion of the Sevier hinterland—the northern Ruby Mountains–East Humboldt Range and Wood Hills, northeastern Nevada: Tectonics, v. 11, p. 154–164.

Howard, K.A., 1966, Structure of the metamorphic rocks of the northern Ruby Mountains, Nevada: New Haven: Yale University, Ph.D. dissertation, vi + 170 p.

Howard, K.A., 1971, Paleozoic metasediments in the northern Ruby Mountains, Nevada: Geological Society of America Bulletin, v. 82, p. 250–264.

Howard, K.A., 1980, Metamorphic infrastructure in the northern Ruby Mountains, Nevada, *in* Crittenden, M.D., Jr., Coney, P.J., and Davis, G.H. editors, Cordilleran metamorphic core complexes: Geological Society of America Memoir 153, p. 335–347.

Howard, K.A., 2000, Geologic map of the Lamoille quadrangle, Elko County, Nevada: Nevada Bureau of Mines and Geology Map 125, scale: 1:24,000, 4 p.

Howard, K.A., Kistler, R.W., Snoke, A.W., and Willden, R., 1979, Geologic map of the Ruby Mountains, Nevada: U.S. Geological Survey Map I-1136, 1:125,000.

Howard, K.A., and MacCready, T., 2004, Geologic map of the Verdi Peak quadrangle, Elko County, Nevada: Nevada Bureau of Mines and Geology Map 147, scale: 1:24,000, 4 p.

Howard, K.A., Wooden, J.L., Barnes, C.G., Premo, W.R., Snoke, A.W., and Lee, S.-Y., 2011, Episodic growth of a Late Cretaceous and Paleogene intrusive complex of pegmatitic leucogranite, Ruby Mountains core complex, Nevada, USA: Geosphere, v. 7, no. 5, p. 1220–1248; doi:10.1130/GES00668.1.

Hurlow, H.A., 1987, Structural geometry, fabric, and chronology of a Tertiary extensional shear zone-detachment system, southwestern East Humboldt Range, Elko County, Nevada: Laramie, University of Wyoming, M.S. Thesis, ix + 141 p.

Hurlow, H.A., Snoke, A.W., and Hodges, K.V., 1991, Temperature and pressure of mylonitization in a Tertiary extensional shear zone, Ruby Mountains–East Humboldt Range, Nevada—tectonic implications: Geology, v. 19, p. 82–86.

King, C., 1878, Systematic geology—geological exploration of the Fortieth Parallel, v. I: Washington, D.C., U.S. Government Printing Office, 803 p.

Kistler, R.W., Ghent, E.D., and O'Neill, J.R., 1981, Petrogenesis of garnet two-mica granites in the Ruby Mountains, Nevada: Journal of Geophysical Research, v. 86, p. 10,591–10,606.

Laabs, B., Licciardi, J., Leonard, E., Munroe, J., and Marchetti, D., 2020, Updated cosmogenic chronologies of Pleistocene mountain glaciation in the western United States and associated paleoclimate inferences: Quaternary Science Reviews, 242 p.

Lee, S-Y, Barnes, C.G., Snoke, A.W., Howard, K.A., and Frost, C.D., 2003, Petrogenesis of Mesozoic, peraluminous granites in the Lamoille Canyon area, Ruby Mountains, Nevada, USA: Journal of Petrology, v. 44, p. 713–732.

Lister, G.S., and Snoke, A.W., 1984, S-C mylonites: Journal of Structural Geology, v. 6, p. 617–637.

McGrew, A.J., 2018, Geologic map of the Humboldt Peak quadrangle, Elko County, Nevada: Nevada Bureau of Mines and Geology Map 186, scale: 1:24,000, 23 p.

McGrew, A.J., and Snoke, A.W., 2015, Geologic map of the Welcome quadrangle and an adjacent part of the Wells quadrangle, Elko County, Nevada: Nevada Bureau of Mines and Geology Map 184, scale: 1:24,000, 40 p.

McGrew, A.J., Peters, M.T., and Wright, J.E., 2000, Thermobarometric constraints on the tectonothermal evolution of the East Humboldt Range metamorphic core complex, Nevada: Geological Society of America Bulletin, v. 112, p. 45–60.

Miller, D.M., 1983, Allochthonous quartzite sequence in the Albion Mountains, Idaho, and proposed Proterozoic Z and Cambrian correlatives in the Pilot Range, Utah and Nevada, *in* Miller, D. M., Todd, V. R., and Howard, K. A., editors, Tectonics and stratigraphic studies in the eastern Great Basin: Geological Society of America Memoir 157, p. 191–213.

Misch, P., and Hazzard, J.C., 1962, Stratigraphy and metamorphism of late Precambrian rocks in central northeastern Nevada and adjacent Utah: American Association of Petroleum Geologists Bulletin, v. 46, p. 289–343.

Mueller, K.J., 1992, Tertiary basin development and exhumation of the northern East Humboldt-Wood Hills metamorphic core complex, Elko County, Nevada: Laramie, University of Wyoming, Ph.D. dissertation, xv + 205 p.

Rejebian, V.A., Harris, A.G., and Huebner, J.S., 1987, Conodont color and textural alteration—an index to regional, metamorphism, contact metamorphism, and hydrothermal alteration: Geological Society of America Bulletin, v. 99, p. 471–479.

Rey, P.F., Teyssier, C., Kruckenberg, S.C., and Whitney, D.L., 2011, Viscous collision in channel explains double domes in metamorphic core complexes: Geology, v. 39, p. 387–390.

Sharp, R.P., 1938, Pleistocene glaciation in the Ruby-East Humboldt Range, northeastern Nevada: Journal of Geomorphology, v. 1, no. 4, p. 296–323.

Sharp, R.P., 1939, Basin-Range structure of the Ruby-East Humboldt Range, northeastern Nevada: Geological Society of America Bulletin, v. 51, p. 337–372.

Sharp, R.P., 1940, Geomorphology of the Ruby-East Humboldt Range, Nevada: Geological Society of America Bulletin, v. 51, p. 337–372.

Sicard, K.R., 2012, The relationship between Cretaceous and Tertiary magmatism and structural development in the southeastern East Humboldt Range, part of the Ruby-East Humboldt core complex, northeast Nevada: Laramie, University of Wyoming, M.S. Thesis, *xv* + 138 p.

Sicard, K.R., and Snoke, A.W., 2020, Geologic map of the Gordon Creek quadrangle, Elko County, Nevada: Nevada Bureau of Mines and Geology Map 188, scale 1:24,000, 28 p.

Simpson, C., and Schmid, S.M., 1983, An evaluation of criteria to deduce the sense of movement in sheared rocks: Geological Society of America Bulletin, v. 94, p. 1281–1288.

Snelson, S., 1957, The geology of the northern Ruby Mountains and the East Humboldt Range, Elko County, Nevada: Seattle: University of Washington, Ph.D. dissertation, 214 p.

Snoke, A.W., 1980, Transition from infrastructure to suprastructure in the northern Ruby Mountains, Nevada, *in* Crittenden, M.D., Jr., Coney, P.J., and Davis, G.H., editors, Cordilleran metamorphic core complexes: Geological Society of America Memoir 153, p. 287–333.

Snoke, A.W., 1998, Folds and other mesoscopic structural features associated with an extensional mylonitic shear zone, *in* Snoke, A.W., Tullis, J., and Todd, V.R., editors, Fault-related rocks—a photographic atlas: Princeton University Press, p. 360–363.

Snoke, A.W., and Howard, K.A., 1984, Geology of the Ruby Mountains–East Humboldt Range, Nevada—a Cordilleran metamorphic core complex, *in* Lintz, J., Jr., editor, Western geological excursions: Geological Society of America 1984 Annual meeting, v. 4, p. 260–303.

Snoke, A.W., McKee, E.H., and Stern, T.W., 1979, Plutonic, metamorphic, and structural chronology in the northern Ruby Mountains, Nevada—a preliminary report: Geological Society of America Abstracts with Programs, v. 11, no. 7, p. 520–521.

Snoke, A.W., McGrew, A.J., Valasek, P.A., and Smithson, S.B., 1990, A crustal cross section for a terrain of superimposed shortening and extension—Ruby Mountains–East Humboldt Range metamorphic core complex, Nevada, *in* Salisbury, M.H., and Fountain, D.M., editors, Exposed cross sections of the continental crust: Kluwer Academic Publishers, p. 103–135.

Snoke, A.W., Howard, K.A., McGrew, A.J., Burton, B.R., Barnes, C.G., Peters, M.T., and Wright, J.E., 1997, The grand tour of the Ruby-East Humboldt metamorphic core complex, northeastern Nevada: Part 1—Introduction & Road Log, *in* Link, P.K., and Kowallis, B.J., editors, Proterozoic to recent stratigraphy, tectonics, and volcanology, Utah, Nevada, southern Idaho and central Mexico: Brigham Young University Geology Studies, v. 42, Part 1, p. 225–269.

Spencer, J.E., 1984, Role of tectonic denudation in warping and uplift of low-angle normal faults: Geology, v. 12, p. 95–98.

Steele, G., 1960, Pennsylvanian-Permian stratigraphy of the east-central Nevada and adjacent Utah, *in* Eleventh Annual Field Conference Guidebook: Intermountain Association of Petroleum Geologists, p. 91–113.

Stevens, C.H., 1979, Lower Permian of the Cordilleran miogeosyncline: Geological Society of America Bulletin, Part II, v. 90, p. 381–455.

Sullivan, W.A., and Snoke, A.W., 2007, Comparative anatomy of core-complex development in the northeastern Great Basin, U.S.A.: Rocky Mountain Geology, v. 42, p. 1–29.

Taylor, G.K., 1984, Stratigraphy, metamorphism, and structure of the southeastern East Humboldt Range, Elko County, Nevada: University of South Carolina, Columbia, M.S. Thesis, *vii* + 148 p.

Tullis, J., 1983, Deformation of feldspars, *in* Ribbe, P.H., editor, Feldspar mineralogy, reviews in mineralogy, v. 2 (2nd edition): Mineralogical Society of America, p. 297–323.

Valasek, P.A., Snoke, A.W., Hurich, C.A., and Smithson, S.B., 1989, Nature and origin of seismic reflection fabric, Ruby-East Humboldt metamorphic core complex, Nevada: Tectonics, v. 8, p. 391–415.

Wardlaw, B.R., and Collinson, 1978, Stratigraphic relations of Park City group (Permian) in eastern Nevada and western Utah: American Association of Petroleum Geologists Bulletin, v. 62, p. 1171–1184.

Wayne, W.J., 1984, Glacial chronology of the Ruby Mountains–East Humboldt Range, Nevada: Quaternary Research, v. 21, p. 286–303.

Wickham, S.M., and Peters, M.T., 1993, High $\delta^{13}C$ Neoproterozoic carbonate rocks in western North America: Geology, v. 21, p. 165–168.

Woodward, L.A., 1967, Stratigraphy and correlation of Late Precambrian rocks of Pilot Range, Elko County, Nevada and Box Elder County, Utah: American Association of Petroleum Geologist Bulletin, v. 51, p. 235–243.

Wright, J.E., and Snoke, A.W., 1993, Tertiary magmatism and mylonitization in the Ruby-East Humboldt metamorphic core complex, northeastern Nevada—U-Pb geochronology and Sr, Nd, Pb isotope geochemistry: Geological Society of America Bulletin, v. 105, p. 935–952.

Zuza, A.V., Dee, S., and Laabs, B.J.C., 2020, Geologic map of the north half of the Tent Mountain quadrangle, Elko County, Nevada: Nevada Bureau of Mines and Geology Open-File Report 20-3, scale 1:24,000, 16 p.

Suggested Citation:

Snoke, A.W., Howard, K.A., and Dee, S., 2021, Geologic map of the Secret Valley quadrangle Elko County, Nevada: Nevada Bureau of Mines and Geology Map 189, scale 1:24,000, 21 p.

© Copyright 2021 The University of Nevada, Reno. All Rights Reserved.

Table 1. Summary of Ar ages of Cenozoic igneous rocks

Sample	Age	Rock type	Map Unit	Analyzed phase	Ag (Ma)	2σ	K/Ca	2σ	n/nt*	Elev. (m)	Lat83	Long83	Source	Note
H14-54	$^{40}Ar/^{39}Ar$	rhyolite lava	Tr	anorthoclase	15.37	0.04	9	1.9	24/25	1984	40.869185	115.246145	Unpublished; C. Henry	single crystal analyses
A	K/Ar	rhyolite lava vitrophyre	Tr	sanidine	15.0	1.5				1976.4	40.871878	115.243683	E.H. McKee, written commun., 1978; reported in Snoke, 1980	

n/nt* -- number of analyses used in calculated age over the total number of analyses